

## Experimental IR and Raman Spectroscopy and DFT Methods Based Material Characterization and Data Analysis of 2- Nitrophenol

Dixit V\* and Yadav RA

Laser and Spectroscopy Laboratory, Department of Physics, Banaras Hindu University, Varanasi -221005, India

### Abstract

Vibrational characteristics of 2- nitrophenol have been investigated using experimental IR and Raman data and computational data using DFT method employing the 6-311++G\*\* basis set available on Gaussian-09 software for the most stable conformer C-1. Complete vibrational assignments of the experimental IR and Raman bands have been proposed in light of the results obtained from the DFT computations and the PEDs computed using GAR2PED software. The optimized geometrical parameters suggest that the overall symmetry of the most stable molecule is Cs. The molecule is expected to have three conformers. In the present article all the characterizations and the analyses of the lowest energy conformer of 2-NP have been studied. The charge transfer occurring in the molecule has been shown by HOMO-LUMO energy orbitals the energy gap of HOMO LUMO orbitals have been found 4.03eV. The mappings of electron density iso-surface with the electrostatic potential (ESP), has been carried out to get the information about the size, shape, charge density distribution and site of chemical reactivity of 2-NP. Current density and magnetic shielding of C-1 have been investigated. Some essential thermo molecular characteristics, namely, enthalpy, Gibb's free energy, thermal energy, entropy, heat capacity, internal energy and the partition functions of the molecule have also been analyzed.

**Keywords:** Optimized structure; Conformers; Entropy; MESP; Magnetic shielding; 2-nitro-phenol

### Introduction

Nitro phenols constitute a class of volatile organic compounds that is increasingly presented in urban as well as in natural environments [1-3]. These are important and versatile compounds in the industrial, agricultural and defence applications [4] and are frequently used as intermediates in the manufacture of explosives, pharmaceuticals, pesticides, pigments, dyes, rubber chemicals, lumber preservatives, photographic chemicals, etc. [5-8]. 2- Nitro-phenols (2-NP), in particular, poses significant health risks since it is a toxic to mammals, microorganisms and anaerobic bacteria. Its toxicity is thought to be due to the nitro group being easily reduced by the enzymes into nitro anion radical, nitroso and hydroxylamine derivatives [4]. Although extensive experimental and theoretical studies are reported on the structural and vibrational studies of mono-substituted phenols [9,10] dealing with their structural features, intra-molecular H-bonding parameters and the vibrational spectra [11-14], only few works of this kind exist on phenols [15-18]. In the present study we report the results of our probing into the application of the DFT based SQM method [19] to the vibrational analysis of hydrogen bonded systems. The main difficulty in such investigations is that the vibrational spectra of these compounds have not been completely analyzed even now and generally only rough assignments are available. Therefore, an investigation of the performance of the DFT-based SQM method has to be carried out simultaneously with a complete vibrational analysis of the molecule. This process was done successfully in the case of 2,6-difluorophenol earlier [20].

The 2-NP molecule, contains a strong intra-molecular (O) H.....O(N) hydrogen bonding interaction which has been analyzed by various experimental and theoretical studies [21-31]. The extensive investigations corresponding to the vibrational description of 2-NP is not complete. Most of the numerous spectroscopic studies [24,31-33] focused on the vibrations from which the information can be carried out about the hydrogen bonding interaction, first of all on the OH stretching and OH torsion.

In the present work calculations have been made for the optimized molecular geometries, APT and Mulliken atomic charges and the fundamental vibrational wave numbers along with their intensities in the IR spectrum, Raman activities and the depolarization ratios of the Raman lines using the DFT (B3LYP) method employing the 6-311++G\*\* basis set [34-38] available with Gaussian-09 software [39] for the lowest energy conformer C-1 of 2-NP. The experimental IR and Raman spectral data have been analyzed in the light of the computed fundamentals and the corresponding PEDs calculated, using the GAR2PED software [40]. For the calculation of the PEDs the vibrational problem was set up in terms of the internal coordinates for the GAR2PED software. HOMO-LUMO, total density plots, electrostatic potential (ESP) surface and their arrays have been investigated. The essential NLO as well as thermo molecular parameters have been investigated and using NMR analysis employing Continuous Set of Gauge Transformation (CSGT) method electro-magnetic characteristics of 2-NP have been investigated.

### Experimental Detail

One to two milligrams of the pure (98%), a yellow crystalline solid in powdered form, 2-nitro phenol, purchased from Sigma Aldrich Chemical Co. (USA), was used to record the Raman spectra using a home assembled micro-Raman spectrometer: Horiba Jobin-Yuon Spectrometer (iHR-320) system with an inverted microscope (Nikon Eclipse Ti-U, Japan). A Diode laser (Star bright Diode Laser, Torsana Laser Tech, Denmark) of  $\lambda=785$  nm used as source to illuminate the

\*Corresponding author: V. Dixit, Laser and Spectroscopy Laboratory, Department of Physics, Banaras Hindu University, Varanasi-221005, India, Tel: +91 8601463836; Fax: +91 542 2368390; E-mail: [vikazimp@rediffmail.com](mailto:vikazimp@rediffmail.com), [drvikasbhu@gmail.com](mailto:drvikasbhu@gmail.com)

Received July 23, 2015; Accepted August 17, 2015; Published August 26, 2015

Citation: Dixit V, Yadav RA (2015) Experimental IR and Raman Spectroscopy and DFT Methods Based Material Characterization and Data Analysis of 2- Nitrophenol. Biochem Pharmacol (Los Angel) 4: 183. doi:10.4173/2167-0501.1000183

Copyright: © 2015 Dixit V, et al. This is an open-access article distributed under the terms of the Creative Commons Attribution License, which permits unrestricted use, distribution, and reproduction in any medium, provided the original author and source are credited.

sample sandwiched between quartz cover slip and borosilicate glass slide. The sample was mounted on the microscope stage and a 60X microscope objective have been used to focus the laser beam and to record the Raman signals. A liquid Nitrogen cooled Symphony CCD detector have been utilized to collect the Raman scattered radiation. The spectral range of the micro-Raman have been kept 200-3100  $\text{cm}^{-1}$  with resolution 5  $\text{cm}^{-1}$ , accuracy 2  $\text{cm}^{-1}$  at spectrometer slit width 100  $\mu\text{m}$ . In order to record a better Raman spectrum, data were obtained using a laser power of 47mW with the acquisition times of 5 min.

FTIR spectrum of 2-NP sample was recorded using KBr pellet. The 10 mg of the 2-NP sample was weighed and properly mixed with 990 mg KBr. This mixture was then pelleted using KBr pellet maker by applying pressure using 8 tons weight for half an hour. FTIR spectrum was recorded using the above mentioned pellet at room temperature, using an FTIR spectrometer (Jasco 6300) with a standard source. The spectra have been recorded in the range of 400- 4000  $\text{cm}^{-1}$ . The 200 scans have been taken with 2  $\text{cm}^{-1}$  spectral resolution for all the three samples.

## Computational Details

To optimize the structure of 2-NP the following procedure was adopted. Initially the benzene ring (including H atoms only) was optimized. After this an OH group was added to a carbon atom of benzene ring and the structure was optimized. With this structure a nitro group was added to the ortho position of phenolic group (Figure 1).

This structure was further optimized. In the optimized structure if hydrogen atom of the OH group faces the  $\text{NO}_2$  group the structure remains planar. However, if the hydrogen atom of the OH group is kept away from the  $\text{NO}_2$  group there are two possible conformers of 2-NP, in one conformer the plane of  $\text{NO}_2$  makes the angle -33.70 while in the other it makes an angle of 33.70 with the plane of phenyl ring (Figure 2).

Therefore total 3 possible conformers have been found to exist of the 2-NP molecule. The energies of all the three optimized conformers are -512.12911314 (C-1), -512.11232617 (C-2) and -512.10755721(C-3) a.u. (Table 1). In the present paper we have considered the vibrational characteristics of the most stable conformer C-1 only.

The optimized molecular geometries, APT charges and the fundamental vibrational wave numbers along with their corresponding intensities in IR spectrum, Raman activities and the depolarization ratios of the Raman bands for the present molecule were computed at the B3LYP/6-311++G\*\* level using the Gaussian 09 program package. The unscaled B3LYP/6-311++G\*\* vibrational frequencies are generally slightly larger than the experimental values. In order to achieve the reasonable frequency matching, the scale factors proposed by Rauhut and Pulay [42] were employed. The assignments of all the normal modes of vibration have been made on the basis of the computed PEDs. The experimental IR and Raman frequencies corresponding to the fundamental modes have been compared with the calculated fundamental frequencies in light of the PEDs. The molecular electrostatic potential (ESP) surface, used for the predicting sites and relative reactivity towards the electrophilic attack and in the studies of biological recognition and hydrogen bonding interactions, has been plotted and the complete thermo-molecular data analysis, complete

description of global reactivity parameters and essential features of electro-magnetism of 2-NP have been investigated.

## Results and Discussions

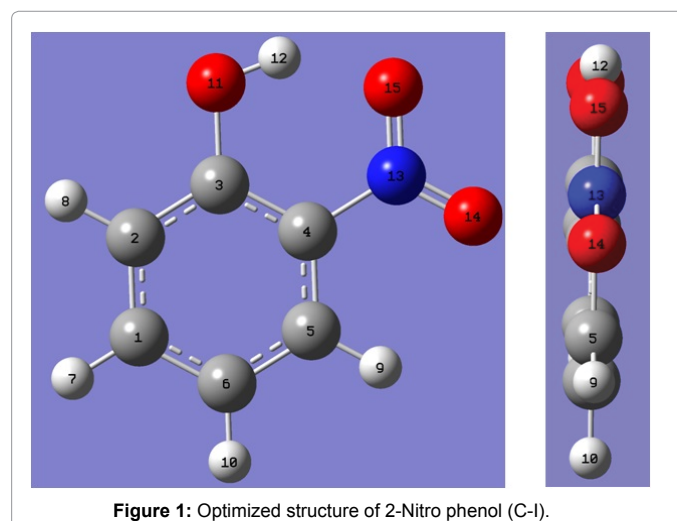
### Molecular geometries

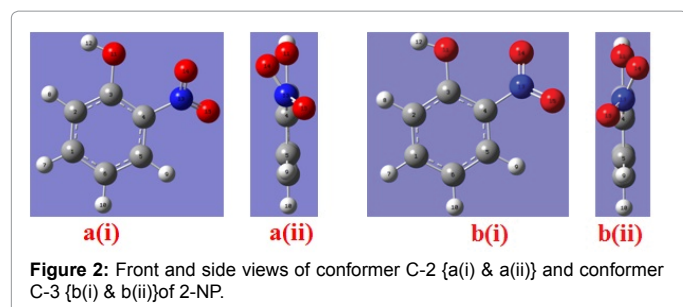
The geometrical parameters of 2-NP computed at the B3LYP/6-311G\*\* level of theory are compared with the experimental and MP2/6-31G\* data in Table 2. The optimized geometrical structure of 2-NP has overall Cs symmetry for the lowest energy conformer. The computed O-H and N-O bond lengths are larger compared with the experimental values. At the same time, the C-O and C-N bond lengths seem to be somewhat shorter. These geometrical parameters are sensitive to hydrogen bonding [15]. Taking into account the above considerations, the data (Table 2) show good agreement between the experimental and theoretical geometries with some minor discrepancies. The computed O-H and N-O bond lengths are larger compared to the experimental values. The computed bond angles are consistent at both levels (Electron Diffraction and MP2/6-31G\*) of theory; the deviations from the experimental values are within or close to experimental error.

The bond lengths of  $\text{C}_1\text{-C}_2$ ,  $\text{C}_3\text{-O}_{11}$ ,  $\text{C}_4\text{-N}_{13}$  and  $\text{C}_5\text{-C}_6$  respectively are shorter while those lengths of  $\text{C}_1\text{-C}_6$ ,  $\text{C}_2\text{-C}_3$ ,  $\text{C}_3\text{-C}_4$ ,  $\text{C}_4\text{-C}_5$  and  $\text{O}_{11}\text{-H}_{12}$  respectively are found to be larger in the most stable conformer than both the C-1 and C-2 conformers. Also, angle  $\alpha$  ( $\text{C}_4\text{-C}_3\text{-O}_{11}$ ) is found to be larger while angle  $\alpha$  ( $\text{O}_{14}\text{-N}_{13}\text{-O}_{15}$ ) is found to be shorter in the most stable conformer than the other two (Table 2). These conformational discrepancies may be due to intra-molecular hydrogen bonding in the most stable conformer and also due to instability of conformers C-2 and C-3 respectively.

### APT charges

Atomic polarizability tensor (APT) charge is interpreted as the sum of charge tensor and charge flux tensor, leading to a charge-charge flux model [43,44]. The APT atomic charges (in unit of e) at various atomic sites of 2-NP are collected in Table 3. The carbon atoms belonging to the ring have alternately positive and negative APT charges with different magnitudes. All the H and N atoms have positive APT charges with different magnitudes, while the O atoms possess negative and different magnitudes of APT charges. The N atom possesses the highest magnitude which is connected directly to the ring and the two O atoms. It is also noticeable that the magnitude of the APT charge on





C<sub>3</sub> attached to the OH group is the largest of all the C atoms. Also, it is interesting to note that the N atom possesses positive APT charge. The magnitude of the APT charge on H<sub>12</sub> is the largest of all the H atoms. The O atoms possess almost equal APT charges.

### Mulliken atomic charges

Mulliken atomic charge calculation plays an important role in the application of quantum chemical calculation to molecular systems, because the atomic charges affect the dipole moment, polarizability, electronic structure, and much more properties of the molecular systems. Mulliken atomic charges (in unit of e) at various atomic sites of 2-NP are collected in Table 3 from which it can be noticed that all the carbon atoms except C<sub>4</sub> and C<sub>5</sub>, have negative Mulliken atomic charges. One of the O atoms attached to the N atom with a single bond possesses positive Mulliken atomic charge. However, it is an electronegative atom like N and O atoms. The H atoms possess positive Mulliken atomic charge. The Mulliken atomic charge at the C atom attached to the OH group is the largest of all the C atoms and the H atom of the OH group possesses the largest Mulliken atomic charge of all the H atoms in the C-1 conformer.

### ESP charges

The studies of effective atomic charges play a crucial role in the application of quantum mechanical computations to the molecular systems. Despite the conceptual problems associated with the dividing up overall molecular charge density in atomic contributions, and all the conventional problems related to the finding of convenient and robust algorithm applicable to a wide range of the systems [45]. The beauty of effective atomic charges as the parameters for the calculation of electrostatic interactions in a various molecular mechanics simulation packages is certainly one essential area of application. Partial atomic charges play a different, but even more important, role in the qualitative rationalization of organic and inorganic reactivity [46]. The molecular electrostatic potential (ESP) derived charges are those are reproduced by fitting the partial atomic charges to reproduce the molecular electrostatic potential (MEP) at a number of points around the molecule at a (large) number of grid points using Merge-Singh-Kollman (MK) scheme [47].

The molecular ESP derived charges at various atomic sites of 2-NP have been contained in the Table 3. Clearly, the ESP charges at all the

C atoms except C<sub>3</sub>, have negative and small but different value while C<sub>3</sub> atom, attached to OH group of 2-NP, have positive and largest value amongst all the C atoms of 2-NP. All the H atoms on the ring possess smaller but positive ESP charges while H atom of OH group attains positive and largest value of all the H atoms in the molecule. The O atoms possess negative ESP charges. The O atom of OH group attains largest negative value (-0.590398 e) while N atom of NO<sub>2</sub> group attains largest positive value (0.681548 e) of ESP charges in 2-NP.

### Vibrational assignments

The 2-NP molecule is a 15 atomic molecule with 39 normal modes of vibration in which 30 modes are associated with the benzene ring which are : 12 stretching modes - $\nu$ , 3 planar ring deformation - $\alpha(R)$ , 3 non planar ring deformation - $\Phi(R)$ , 6 planar deformation modes - $\beta(C-H)$  and 6 non-planar deformation modes - $\gamma(C-H)$ , out of which 2 of each i.e.  $\beta(C-H)$  and  $\gamma(C-H)$  become  $\beta(C-N)$ ,  $\beta(C-O)$  and  $\gamma(C-N)$ ,  $\gamma(C-O)$  respectively. The three normal modes of OH-group are: OH stretching - $\nu(OH)$ , OH torsion - $\tau(OH)$  and C-O-H angle bending. The six normal modes of the nitro group are: anti-symmetric NO<sub>2</sub> stretching - $\nu_{as}(NO_2)$ , symmetric NO<sub>2</sub> stretching - $\nu_s(NO_2)$ , NO<sub>2</sub> rocking - $\rho(NO_2)$ , NO<sub>2</sub> wagging - $\omega(NO_2)$ , NO<sub>2</sub> scissoring - $\delta(NO_2)$  and NO<sub>2</sub> torsion - $\tau(NO_2)$ .

The calculated and observed vibrational frequencies along with the corresponding PEDs and vibrational assignments are collected in Table 4. The experimental and calculated IR and Raman spectra are reproduced in Figure 3-6. The normal mode assignments have been discussed under the following sections: (i) The phenyl ring modes (30), (ii) The OH group modes (3) and (iii) The NO<sub>2</sub> group modes (6).

**Phenyl ring modes (30):** The four C-H stretching modes  $\nu$  (C-H) are assigned to the frequencies 3034 ( $\nu_5$ ), 3181 ( $\nu_4$ ), 3186 ( $\nu_3$ ) and 3205 ( $\nu_2$ ) cm<sup>-1</sup> which correspond dominantly to the modes  $\nu(C_1-H_7)$ ,  $\nu(C_6-H_{10})$ ,  $\nu(C_2-H_8)$  and  $\nu(C_5-H_9)$  respectively. The C-H stretching modes  $\nu$  (C-H) were assigned to the frequencies 3070, 3088, 3096 and 3117 cm<sup>-1</sup> [41] and also to the frequencies 3208, 3229 and 3245 cm<sup>-1</sup> [48]. The C-H stretching vibrations are pure and highly localized modes. There are 6 C-C stretching modes  $\nu(R)$  due to the phenyl ring which are identified as the computed frequencies 1002 ( $\nu_{19}$ ), 1051 ( $\nu_{18}$ ), 1306 ( $\nu_{12}$ ), 1420 ( $\nu_{10}$ ), 1547 ( $\nu_7$ ), 1586 ( $\nu_6$ ) cm<sup>-1</sup>. These modes are strongly coupled with many other modes. These modes were assigned to the frequencies 1020, 1581 and 1620 cm<sup>-1</sup> [41] and also to the frequencies 1369, 1551, 1584 and 1612 cm<sup>-1</sup> [48]. The C-N and C-O stretching modes occur at frequencies 667 ( $\nu_{28}$ ), 1442 ( $\nu_9$ ) cm<sup>-1</sup> corresponding to the modes  $\nu(C_4-N_{13})$  and  $\nu(C_3-O_{11})$  respectively. These modes are also coupled with many other modes. The C-O stretching mode in the literature was found to be corresponding to the frequency 1269 [41] and 1464 cm<sup>-1</sup> [48].

There are three ring planar deformation modes which we assign as the frequencies 865 ( $\nu_{22}$ ), 559 ( $\nu_{30}$ ) and 373 ( $\nu_{35}$ ) cm<sup>-1</sup>. These modes are coupled with other modes as shown in the Table-4. The three ring non-planar deformation modes are correlated to the frequencies 657 ( $\nu_{29}$ ), 413 ( $\nu_{34}$ ) and 141 ( $\nu_{38}$ ) cm<sup>-1</sup> corresponding to modes 4 and 16(a,b) of the

Conformers	Point group	Total energy (Hartree)	Relative energy		
			Hartree	Temp. (K)	kcal/mol
C-1	C <sub>s</sub>	-512.12911314	0	0	0
C-2	C <sub>1</sub>	-512.11232617	0.01678697	5300.9405365	10.533984965
C-3	C <sub>1</sub>	-512.10755721	0.02155593	6806.868848	13.52655319

**Table 1:** Total and relative energies of all the possible conformers of 2-NP.

S.No.	Parameters	B3-LYP/6-311++G**			ED <sup>®</sup>	MP2(FC) / 6-31G* <sup>®</sup>
		C-1 <sup>§</sup> #	C-2 <sup>#</sup>	C-3 <sup>#</sup>		
1	r(C <sub>1</sub> -C <sub>2</sub> )	1.382	1.389	1.389	1.388	1.387
2	r(C <sub>1</sub> -C <sub>6</sub> )	1.404	1.396	1.396	1.399	1.402
3	r(C <sub>1</sub> -H <sub>7</sub> )	1.084	1.084	1.084	1.089	1.086
4	r(C <sub>2</sub> -C <sub>3</sub> )	1.404	1.400	1.400	1.406	1.405
5	r(C <sub>2</sub> -H <sub>8</sub> )	1.083	1.086	1.086	1.089	1.086
6	r(C <sub>3</sub> -C <sub>4</sub> )	1.415	1.405	1.405	1.411	1.410
7	r(C <sub>3</sub> -O <sub>11</sub> )	1.336	1.352	1.352	1.359	1.351
8	r(C <sub>4</sub> -C <sub>5</sub> )	1.402	1.393	1.393	1.402	1.401
9	r(C <sub>4</sub> -N <sub>13</sub> )	1.453	1.473	1.473	1.464	1.456
10	r(C <sub>5</sub> -C <sub>6</sub> )	1.380	1.387	1.387	1.387	1.386
11	r(C <sub>5</sub> -H <sub>9</sub> )	1.081	1.082	1.082	1.089	1.086
12	r(C <sub>6</sub> -H <sub>10</sub> )	1.082	1.082	1.082	1.089	1.086
13	r(O <sub>11</sub> -H <sub>12</sub> )	0.982	0.964	0.964	0.969	0.986
14	r(N <sub>13</sub> -O <sub>14</sub> )	1.219	1.221	1.221	1.225	1.239
15	r(N <sub>13</sub> -O <sub>15</sub> )	1.248	1.228	1.228	1.241	1.255
16	α(C <sub>2</sub> -C <sub>1</sub> -C <sub>6</sub> )	121.031	120.5	120.5	122.9	120.5
17	α(C <sub>2</sub> -C <sub>1</sub> -H <sub>7</sub> )	119.217	119.3	119.3	--	--
18	α(C <sub>6</sub> -C <sub>1</sub> -H <sub>7</sub> )	119.752	120.2	120.2	--	--
19	α(C <sub>1</sub> -C <sub>2</sub> -C <sub>3</sub> )	120.786	121.0	121.0	118.1	121.1
20	α(C <sub>1</sub> -C <sub>2</sub> -H <sub>8</sub> )	121.644	120.2	120.2	--	--
21	α(C <sub>3</sub> -C <sub>2</sub> -H <sub>8</sub> )	117.570	118.8	118.8	--	--
22	α(C <sub>2</sub> -C <sub>3</sub> -C <sub>4</sub> )	117.659	117.8	117.8	119.4	117.4
23	α(C <sub>2</sub> -C <sub>3</sub> -O <sub>11</sub> )	117.741	122.0	122.0	--	--
24	α(C <sub>4</sub> -C <sub>3</sub> -O <sub>11</sub> )	124.600	120.2	120.2	123.9	125.6
25	α(C <sub>5</sub> -C <sub>4</sub> -C <sub>6</sub> )	121.165	121.1	121.1	121.4	121.7
26	α(C <sub>3</sub> -C <sub>4</sub> -N <sub>13</sub> )	120.816	121.5	121.5	120.8	121.0
27	α(C <sub>5</sub> -C <sub>4</sub> -N <sub>13</sub> )	118.019	117.4	117.4	--	--
28	α(C <sub>4</sub> -C <sub>5</sub> -C <sub>6</sub> )	119.999	120.3	120.3	119.0	119.6
29	α(C <sub>4</sub> -C <sub>5</sub> -H <sub>9</sub> )	118.254	118.2	118.2	--	--
30	α(C <sub>6</sub> -C <sub>5</sub> -H <sub>9</sub> )	121.747	121.5	121.5	--	--
31	α(C <sub>1</sub> -C <sub>6</sub> -C <sub>5</sub> )	119.360	119.2	119.2	119.3	119.7
32	α(C <sub>1</sub> -C <sub>6</sub> -H <sub>10</sub> )	120.505	120.7	120.7	--	--
33	α(C <sub>5</sub> -C <sub>6</sub> -H <sub>10</sub> )	120.135	120.1	120.1	--	--
34	α(C <sub>3</sub> -O <sub>11</sub> -H <sub>12</sub> )	107.393	109.5	109.5	104.4	106.8
35	α(C <sub>4</sub> -N <sub>13</sub> -O <sub>14</sub> )	119.320	118.1	118.1	118.2	118.4
36	α(C <sub>4</sub> -N <sub>13</sub> -O <sub>15</sub> )	117.914	116.9	116.9	118.6	118.8
37	α(O <sub>14</sub> -N <sub>13</sub> -O <sub>15</sub> )	122.766	124.9	124.9	123.3	122.8
38	δ(C <sub>6</sub> -C <sub>1</sub> -C <sub>2</sub> -C <sub>3</sub> )	0.004	0.8	-0.8	--	--
39	δ(C <sub>6</sub> -C <sub>1</sub> -C <sub>2</sub> -H <sub>8</sub> )	179.999	-179.0	179.0	--	--
40	δ(H <sub>7</sub> -C <sub>1</sub> -C <sub>2</sub> -C <sub>3</sub> )	179.997	-179.6	179.6	--	--
41	δ(H <sub>7</sub> -C <sub>1</sub> -C <sub>2</sub> -H <sub>8</sub> )	-0.008	0.6	-0.6	--	--
42	δ(C <sub>2</sub> -C <sub>1</sub> -C <sub>6</sub> -C <sub>5</sub> )	-0.011	0.0	-0.0	--	--
43	δ(C <sub>2</sub> -C <sub>1</sub> -C <sub>6</sub> -H <sub>10</sub> )	180.001	179.9	-179.9	--	--
44	δ(H <sub>7</sub> -C <sub>1</sub> -C <sub>6</sub> -C <sub>5</sub> )	-180.004	-179.7	179.8	--	--
45	δ(H <sub>7</sub> -C <sub>1</sub> -C <sub>6</sub> -H <sub>10</sub> )	0.008	0.2	-0.2	--	--
46	δ(C <sub>1</sub> -C <sub>2</sub> -C <sub>3</sub> -C <sub>4</sub> )	-0.004	-0.4	0.4	--	--
47	δ(C <sub>1</sub> -C <sub>2</sub> -C <sub>3</sub> -O <sub>11</sub> )	-180.000	-178.4	178.4	--	--
48	δ(H <sub>8</sub> -C <sub>2</sub> -C <sub>3</sub> -C <sub>4</sub> )	-179.999	179.4	-179.4	--	--
49	δ(H <sub>8</sub> -C <sub>2</sub> -C <sub>3</sub> -O <sub>11</sub> )	0.004	1.4	-1.4	--	--
50	δ(C <sub>2</sub> -C <sub>3</sub> -C <sub>4</sub> -C <sub>5</sub> )	0.011	-0.8	0.8	--	--
51	δ(C <sub>2</sub> -C <sub>3</sub> -C <sub>4</sub> -N <sub>13</sub> )	-180.029	179.3	-179.3	--	--
52	δ(O <sub>11</sub> -C <sub>3</sub> -C <sub>4</sub> -C <sub>5</sub> )	180.007	177.3	-177.3	--	--
53	δ(O <sub>11</sub> -C <sub>3</sub> -C <sub>4</sub> -N <sub>13</sub> )	-0.033	-2.7	2.7	--	--
54	δ(C <sub>2</sub> -C <sub>3</sub> -O <sub>11</sub> -H <sub>12</sub> )	180.028	2.2	-2.1	--	--
55	δ(C <sub>4</sub> -C <sub>3</sub> -O <sub>11</sub> -H <sub>12</sub> )	0.032	-175.8	175.9	--	--
56	δ(C <sub>3</sub> -C <sub>4</sub> -C <sub>5</sub> -C <sub>6</sub> )	-0.018	1.5	-1.5	--	--
57	δ(C <sub>3</sub> -C <sub>4</sub> -C <sub>5</sub> -H <sub>9</sub> )	-180.007	-178.6	178.6	--	--
58	δ(N <sub>13</sub> -C <sub>4</sub> -C <sub>5</sub> -C <sub>6</sub> )	180.020	178.5	178.5	--	--
59	δ(N <sub>13</sub> -C <sub>4</sub> -C <sub>5</sub> -H <sub>9</sub> )	0.031	1.4	-1.4	--	--

60	$\delta$ (C <sub>3</sub> -C <sub>4</sub> -N <sub>13</sub> -O <sub>14</sub> )	180.052	-33.7	33.7	--	--
61	$\delta$ (C <sub>3</sub> -C <sub>4</sub> -N <sub>13</sub> -O <sub>15</sub> )	0.050	147.8	-147.8	--	--
62	$\delta$ (C <sub>3</sub> -C <sub>4</sub> -N <sub>13</sub> -O <sub>14</sub> )	0.013	146.3	-146.3	--	--
63	$\delta$ (C <sub>3</sub> -C <sub>4</sub> -N <sub>13</sub> -O <sub>15</sub> )	180.011	-32.1	32.1	--	--
64	$\delta$ (C <sub>4</sub> -C <sub>5</sub> -C <sub>6</sub> -C <sub>1</sub> )	0.017	-1.1	1.1	--	--
65	$\delta$ (C <sub>4</sub> -C <sub>5</sub> -C <sub>6</sub> -H <sub>10</sub> )	-179.994	179.0	-179.0	--	--
66	$\delta$ (H <sub>9</sub> -C <sub>5</sub> -C <sub>6</sub> -C <sub>1</sub> )	180.006	179.0	-179.0	--	--
67	$\delta$ (H <sub>9</sub> -C <sub>5</sub> -C <sub>6</sub> -H <sub>10</sub> )	-0.006	-0.9	0.9	--	--

<sup>§</sup> Conformer C-1 is the lowest energy conformer of 2-NP; <sup>\*</sup> Our Work; <sup>®</sup> Ref. 1

**Table 2:** Computed and observed geometrical parameters of 2- NP.

Atoms	APT charges		Mulliken atomic charges		ESP charges		ESP Potentials	
	(C-1)	(C-2/C-3)	(C-1)	C-2/C-3)	(C-1)	C-2/C-3)	C-1	C-2/C-3)
C <sub>1</sub>	0.168082	0.109390	-0.251868	-0.187756	-0.087841	-0.070392	-14.73524	-14.73734
C <sub>2</sub>	-0.168431	-0.166562	-0.165953	0.112368	-0.242264	-0.276459	-14.74573	-14.73986
C <sub>3</sub>	0.617390	0.569682	-0.630033	-0.280495	0.387901	0.311740	-14.66298	-14.66522
C <sub>4</sub>	-0.369569	-0.186726	0.559561	-0.248181	-0.069178	0.011254	-14.69304	-14.70101
C <sub>5</sub>	0.098974	0.070105	0.139598	0.278052	-0.166961	-0.210985	-14.73417	-14.73785
C <sub>6</sub>	-0.238821	-0.186101	-0.249269	-0.259811	-0.137599	-0.132966	-14.74581	-14.74815
H <sub>7</sub>	0.051609	0.049260	0.175404	0.172879	0.138456	0.134908	-1.07628	-1.07627
H <sub>8</sub>	0.067916	0.037818	0.205976	0.138330	0.181123	0.149018	-1.07645	-1.06388
H <sub>9</sub>	0.102578	0.094642	0.239102	0.231315	0.166468	0.186660	-1.07216	-1.07586
H <sub>10</sub>	0.049672	0.048614	0.185472	0.174564	0.136537	0.133989	-1.08086	-1.08272
O <sub>11</sub>	-0.726207	-0.645764	-0.185498	-0.177027	-0.590398	-0.522159	-22.31645	-22.30600
H <sub>12</sub>	0.390488	0.297918	0.290132	0.270747	0.471626	0.417133	-0.95701	-0.94374
N <sub>13</sub>	1.350233	1.219919	-0.296760	-0.207132	0.681548	0.736291	-18.13866	-18.15683
O <sub>14</sub>	-0.688853	-0.677157	0.004956	-0.034067	-0.388638	-0.452560	-22.32424	-22.34426
O <sub>15</sub>	-0.705060	-0.635038	-0.020819	0.016214	-0.480781	-0.415470	-22.32304	-22.34320

\*Charges are in the unit of e

**Table 3:** APT, Mulliken and ESP fitted (MK scheme) atomic charges and molecular electrostatic potentials at different atomic sites of 2-NP (C-1).

t	Calculated Frequencies (cm <sup>-1</sup> )		Observed Freq <sup>®</sup> . (cm <sup>-1</sup> )				PEDs	Mode Assigned
			Ref-[41]		Our work			
	Sc.	Unsc.	Raman	IR	Raman	IR		
v <sub>1</sub>	3453	3471(241,108)0.14	--	3253	--	3358	v(O <sub>11</sub> -H <sub>12</sub> ) (100)	v(O-H)
v <sub>2</sub>	3205	3222(4,94)0.16	--	3115 <sup>*</sup>	--	--	v(C <sub>2</sub> -H <sub>8</sub> ) (91) + v(C <sub>6</sub> -H <sub>10</sub> ) (8)	v(C-H)
v <sub>3</sub>	3186	3203(2,170)0.12	--	3099	--	--	v(C <sub>2</sub> -H <sub>8</sub> ) (67) + (C <sub>1</sub> -H <sub>7</sub> ) (17) + v(C <sub>6</sub> -H <sub>10</sub> ) (12)	v(C-H)
v <sub>4</sub>	3181	3197(5,88)0.62	--	3091	--	3136	v(C <sub>6</sub> -H <sub>10</sub> ) (67) + (C <sub>2</sub> -H <sub>8</sub> ) (23)	v(C-H)
v <sub>5</sub>	3034	3178(4,73)0.65	3100	3060	--	3065	v(C <sub>1</sub> -H <sub>7</sub> ) (78)+v(C <sub>6</sub> -H <sub>10</sub> ) (13)+ v(C <sub>2</sub> -H <sub>8</sub> ) (9)	v(C-H)
v <sub>6</sub>	1586	1661(133,9)0.75	1615	1625	--	1600	v(C <sub>3</sub> -C <sub>4</sub> )(15) + (C <sub>1</sub> -C <sub>2</sub> )(13) + v(C <sub>4</sub> -C <sub>5</sub> )(13) + v(C <sub>1</sub> -C <sub>2</sub> )(13) + v(N <sub>13</sub> -O <sub>14</sub> ) (6)+ α <sub>3</sub> (R)(9)	v(R)
v <sub>7</sub>	1547	1620(81,31)0.56	1600	1603	1582	1559	v(C <sub>5</sub> -C <sub>6</sub> )(21) + v(C <sub>2</sub> -C <sub>3</sub> )(18) + v(C <sub>1</sub> -C <sub>2</sub> )(7) + v(C <sub>4</sub> -C <sub>5</sub> )(6) + v(C <sub>3</sub> -C <sub>4</sub> )(6) + α(C <sub>3</sub> -O <sub>11</sub> -H <sub>12</sub> )(10) + α <sub>2</sub> (R)(9)	v(R)
v <sub>8</sub>	1511	1582(163,37)0.60	1540	1550	1525	1501	v <sub>as</sub> (NO <sub>2</sub> ) (52) + (C <sub>1</sub> -C <sub>2</sub> )(8) + v(C <sub>3</sub> -C <sub>4</sub> )(7) + β(C <sub>4</sub> -N <sub>13</sub> ) (8) + ρ(NO <sub>2</sub> ) (8)	v <sub>as</sub> (NO <sub>2</sub> )
v <sub>9</sub>	1442	1510(119,2)0.30	1465	1476	--	1462	v(C <sub>3</sub> -O <sub>11</sub> ) (13) + (C <sub>1</sub> -C <sub>2</sub> ) (11) + v(C <sub>2</sub> -C <sub>3</sub> )(9) + v(C <sub>4</sub> -C <sub>5</sub> )(7) + β(C <sub>1</sub> -H <sub>7</sub> ) (11) + β(C <sub>5</sub> -H <sub>9</sub> ) (13) + β(C <sub>2</sub> -H <sub>8</sub> ) (17)	v(C-O)
v <sub>10</sub>	1420	1487(107,8)0.44	--	1460 <sup>*</sup>	1453	1423	v(C <sub>1</sub> -C <sub>6</sub> )(12) + v(C <sub>4</sub> -C <sub>5</sub> )(4) + v(C <sub>3</sub> -C <sub>4</sub> )(3) + v <sub>as</sub> (NO <sub>2</sub> ) (26) + β(C <sub>6</sub> -H <sub>10</sub> ) (20) + α(C <sub>3</sub> -O <sub>11</sub> -H <sub>12</sub> ) (6)	v(R)
v <sub>11</sub>	1349	1413(68,40)0.16	1398	1380	1366	1404	α(C <sub>3</sub> -O <sub>11</sub> -H <sub>12</sub> ) (28) + v(C <sub>3</sub> -C <sub>4</sub> )(10) + v(C <sub>1</sub> -C <sub>2</sub> )(9) + v(C <sub>1</sub> -C <sub>6</sub> ) (8) + v(C <sub>2</sub> -C <sub>3</sub> )(6) + v <sub>s</sub> (NO <sub>2</sub> ) (9) + β(C <sub>1</sub> -H <sub>7</sub> ) (9) + β(C <sub>5</sub> -H <sub>9</sub> ) (7)	α(C-O-H)
v <sub>12</sub>	1306	1368(86,3)0.53	1319	1333 <sup>*</sup>	--	1348	v(C <sub>3</sub> -C <sub>4</sub> )(15)+v(C <sub>5</sub> -C <sub>6</sub> )(11)+v(C <sub>1</sub> -C <sub>2</sub> ) (10)+v(C <sub>4</sub> -C <sub>5</sub> ) (5)+v(C <sub>2</sub> -C <sub>3</sub> )(4)+v(C <sub>3</sub> -O <sub>11</sub> )(13) + β(C <sub>2</sub> -H <sub>8</sub> ) (13) + β(C <sub>6</sub> -H <sub>10</sub> ) (8)	v(R)
v <sub>13</sub>	1260	1319(218,77)0.30	1252	1325 <sup>*</sup>	1234	--	β(C <sub>5</sub> -H <sub>9</sub> ) (13) + v(N <sub>13</sub> -O <sub>15</sub> ) (22) + v(C <sub>1</sub> -C <sub>6</sub> )(9) + v(C <sub>5</sub> -C <sub>6</sub> ) (9) + α(C <sub>3</sub> -O <sub>11</sub> -H <sub>12</sub> ) (12) + v(C <sub>4</sub> -N <sub>13</sub> ) (8) + δ(NO <sub>2</sub> ) (6) + v(C <sub>3</sub> -O <sub>11</sub> ) (6)	β(C-H)
v <sub>14</sub>	1226	1284(175,98)0.23	1198	1256 <sup>*</sup>	1181	1284	v <sub>s</sub> (NO <sub>2</sub> ) (24) + v(C <sub>3</sub> -O <sub>11</sub> ) (22) + v(C <sub>4</sub> -C <sub>5</sub> )(9) + v(C <sub>1</sub> -C <sub>6</sub> )(7) + β(C <sub>1</sub> -H <sub>7</sub> ) (7) + δ(NO <sub>2</sub> ) (7)	v <sub>s</sub> (NO <sub>2</sub> )

V <sub>15</sub>	1177	1232(107,42)0.22	1160	1201	1158	1209	$\beta(C_2-H_8)(19) + v(C_4-C_5)(10) + v(C_5-C_6)(8) + v(C_1-C_6)(5) + \alpha(C_3-O_{11}-H_{12})(17) + \beta(C_5-H_9)(10) + v(C_4-N_{13})(7)$	$\beta(C-H)$
V <sub>16</sub>	1131	1185(10,3)0.61	1145	1165	1136	--	$\beta(C_6-H_{10})(43) + \beta(C_5-H_9)(18) + v(C_1-C_2)(11) + v(C_2-C_3)(5) + \beta(C_1-H_7)(12)$	$\beta(C-H)$
V <sub>17</sub>	1106	1158(41,32)0.33	1113	1140	1117	1146	$v(C_3-C_4)(9) + (C_1-C_6)(8) + v(C_1-C_2)(8) + \beta(C_5-H_9)(25) + \beta(C_2-H_8)(19) + v(C_4-N_{13})(11)$	$v(R)$
V <sub>18</sub>	1051	1101(28,4)0.14	1094	1080	--	1092	$v(C_2-C_3)(13) + (C_4-N_{13})(22) + \alpha_1(R)(32) + \beta(C_5-H_9)(9)$	$v(R)$
V <sub>19</sub>	1002	1049(14,26)0.04	1055	1030	1026	1040	$v(C_2-C_3)(47) + (C_3-C_4)(13) + v(C_1-C_2)(7) + \beta(C_2-H_8)(10) + \beta(C_5-H_9)(8)$	$v(R)$
V <sub>20</sub>	978	1000(0,0)0.75	1022	981'	--	1002	$\gamma(C_1-H_7)(51) + \gamma(C_6-H_{10})(18) + \gamma(C_2-H_8)(14) + \Phi_1(R)(11)$	$\gamma(C-H)$
V <sub>21</sub>	956	977(2,0)0.75	998	954	--	973	$\gamma(C_5-H_9)(53) + \gamma(C_6-H_{10})(21) + \gamma(C_2-H_8)(11) + \Phi_2(R)(7) + \gamma(C_1-H_7)(6)$	$\gamma(C-H)$
V <sub>22</sub>	865	884(17,4)0.18	883	871	867	882	$\alpha_1(R)(37) + \alpha_3(R)(8) + \delta(NO_2)(29) + v(C_4-N_{13})(7) + v(C_3-O_{11})(6)$	$\alpha(R)$
V <sub>23</sub>	849	868(0,0)0.75	--	860'	--	--	$\gamma(C_2-H_8)(49) + \gamma(C_2-H_8)(17) + \gamma(C_2-H_8)(9) + \gamma(C_3-O_{11})(7) + \Phi_1(R)(6) + \gamma(C_1-H_7)(6)$	$\gamma(C-H)$
V <sub>24</sub>	819	837(9,35)0.07	817	820	818	832	$\delta(NO_2)(32) + v(C_5-C_6)(12) + v(C_4-C_5)(10) + v(C_1-C_6)(5) + v(C_3-O_{11})(11) + \alpha_1(R)(8) + \alpha_3(R)(6)$	$\delta(NO_2)$
V <sub>25</sub>	760	777(48,0)0.75	--	780	--	773	$\gamma(C_6-H_{10})(39) + \gamma(C_5-H_9)(20) + \gamma(C_1-H_7)(17) + \gamma(C_2-H_8)(10)$	$\gamma(C-H)$
V <sub>26</sub>	720	736(43,1)0.75	--	690	--	712	$\tau(C_3-O_{11})(64) + \omega(NO_2)(24) + \gamma(C_4-N_{13})(7)$	$\tau(C-O)$
V <sub>27</sub>	683	698(83,0)0.75	--	697''	--	--	$\omega(NO_2)(47) + \tau(C_3-O_{11})(20) + \Phi_1(R)(17) + \gamma(C_1-H_7)(7)$	$\omega(NO_2)$
V <sub>28</sub>	667	682(9,4)0.20	667	669''	666	--	$v(C_4-N_{13})(9) + \alpha_2(R)(39) + \alpha_3(R)(16) + v(C_5-C_6)(8) + v(C_1-C_2)(5) + \delta(NO_2)(12)$	$v(C-N)$
V <sub>29</sub>	657	671(16,0)0.75	--	--	--	--	$\Phi_1(R)(53) + \gamma(C_3-O_{11})(23) + \gamma(C_4-N_{13})(11)$	$\Phi(R)$
V <sub>30</sub>	559	571(1,12)0.74	581	563'	561	--	$\alpha_2(R)(25) + \alpha_3(R)(10) + \beta(C_4-N_{13})(22) + \rho(NO_2)(16) + v(C_4-C_5)(9) + \beta(C_3-O_{11})(8)$	$\alpha(R)$
V <sub>31</sub>	542	554(8,3)0.14	549	546'	--	554	$\rho(NO_2)(24) + \beta(C_3-O_{11})(20) + \alpha_1(R)(12) + \alpha_3(R)(11) + v(C_4-N_{13})(6)$	$\rho(NO_2)$
V <sub>32</sub>	522	533(8,0)0.75	--	531	--	536	$\gamma(C_3-O_{11})(29) + \Phi_3(R)(32) + \Phi_1(R)(16) + \gamma(C_6-H_{10})(9) + \Phi_2(R)(6)$	$\gamma(C-O)$
V <sub>33</sub>	427	436(2,4)0.56	427	426'	424	437	$\beta(C_3-O_{11})(34) + \rho(NO_2)(33) + \alpha_3(R)(11) + v(C_4-N_{13})(9)$	$\beta(C-O)$
V <sub>34</sub>	413	422(1,0)0.75	--	--	--	401	$\Phi_2(R)(45) + \Phi_3(R)(15) + \gamma(C_4-N_{13})(28)$	$\Phi(R)$
V <sub>35</sub>	373	381(6,1)0.20	--	372'	--	--	$\alpha_3(R)(24) + \alpha_2(R)(6) + \beta(C_3-O_{11})(32) + v(C_4-N_{13})(19) + \rho(NO_2)(7)$	$\alpha(R)$
V <sub>36</sub>	285	291(5,3)0.44	297	285'	284	--	$\beta(C_4-N_{13})(73) + \rho(NO_2)(9)$	$\beta(C-N)$
V <sub>37</sub>	240	245(0,1)0.75	--	251'	--	--	$\gamma(C_4-N_{13})(36) + \Phi_3(R)(20) + \Phi_1(R)(16) + \Phi_1(R)(12) + \gamma(C_2-H_8)(9)$	$\gamma(C-N)$
V <sub>38</sub>	141	144(0,1)0.75	159'	--	--	--	$\Phi_3(R)(44) + \Phi_1(R)(4) + \tau(C_3-O_{11})(24) + \gamma(C_4-N_{13})(20)$	$\Phi(R)$
V <sub>39</sub>	74	76(1,0)0.75	67	85	--	--	$\tau(C_4-N_{13})(74) + \tau(C_3-O_{11})(17)$	$\tau(C-N)$

- \* Calculated wave numbers below 1000 cm<sup>-1</sup> were scaled by the scale factor 0.9786 and those above 1000 cm<sup>-1</sup> by the scale factor 0.9550.
- \* Number outside bracket is frequency in cm<sup>-1</sup> unit, numbers within the bracket are IR intensity and Raman activity and number outside bracket is depolarization ratio.
- \* Gas-phase except where noted [41]. \* in CCl<sub>4</sub> solution [41]. \*\*recorded in Ar-Matrix [41].
- \* The nos. after the modes are the % PED calculated using GAR2PED. The modes with contribution less than 5% are omitted, except v(R),  $\Phi(R)$  and  $\alpha(R)$ . v = stretching,  $\gamma$  = out-of-plane deformation,  $\beta$  = in-plane deformation,  $\alpha$  = planar ring deformation,  $\Phi$  = non-planar ring deformation,  $\rho(NO_2)$  = rocking of NO<sub>2</sub> group,  $\delta(NO_2)$  = scissoring of NO<sub>2</sub> group,  $\omega(NO_2)$  = wagging of NO<sub>2</sub> group,  $\tau(NO_2)$  = torsion of NO<sub>2</sub> group

**Table 4:** Computed and observed vibrational fundamentals, PEDs and vibrational modes assignments for lowest energy conformer C-1 of 2-NP

benzene molecule. These modes were found to occur at frequencies 152, 297 and 565 cm<sup>-1</sup> [48].

The four C-H planar deformations  $\beta(C-H)$  and four C-H non-planar deformations  $\gamma(C-H)$  are assigned at the frequencies 1106(v<sub>17</sub>), 1177(v<sub>15</sub>), 1260(v<sub>13</sub>), 1131(v<sub>16</sub>), 978(v<sub>20</sub>), 849(v<sub>23</sub>), 956(v<sub>21</sub>) and 760(v<sub>25</sub>) cm<sup>-1</sup> corresponding to the modes  $\beta(C_1-H_7)$ ,  $\beta(C_2-H_8)$ ,  $\beta(C_5-H_9)$ ,  $\beta(C_6-H_{10})$ ,  $\gamma(C_1-H_7)$ ,  $\gamma(C_2-H_8)$ ,  $\gamma(C_5-H_9)$  and  $\gamma(C_6-H_{10})$  respectively. These modes are coupled with many other modes. The modes  $\beta(C-N)$ ,  $\gamma(C-N)$ ,  $\beta(C-O)$  and  $\gamma(C-O)$  correspond to the frequencies 285(v<sub>36</sub>), 240(v<sub>37</sub>), 427 (v<sub>33</sub>) and 522(v<sub>32</sub>) cm<sup>-1</sup> respectively. These modes are strongly coupled modes. The modes  $\beta(C-N)$  and  $\beta(C-O)$  were assigned to the frequencies 298 and 432 cm<sup>-1</sup> [41].

**O-H group modes (3 modes):** The OH stretching  $v(O_{11}-H_{12})$  mode corresponds to the frequency 3453(v<sub>1</sub>) cm<sup>-1</sup>. The O-H stretching vibration is pure and highly localized mode. The O-H stretching

mode was found to correspond to the frequency 3255 [41] and to the frequency 3308 cm<sup>-1</sup> [48]. The torsion of the OH group -  $\tau(C_3-O_{11})$  occurs at frequency 720(v<sub>26</sub>) cm<sup>-1</sup> in our work and at the frequency 711 cm<sup>-1</sup> [41] and is strongly coupled with other modes of vibrations. The C-O-H angle bending-  $\alpha(C_3-O_{11}-H_{12})$  mode is found to correspond to the frequency 1349(v<sub>11</sub>) cm<sup>-1</sup> and also to the frequencies 1377 cm<sup>-1</sup> [41] and 1266/1426 cm<sup>-1</sup> [48], which is also strongly coupled with many modes.

**NO<sub>2</sub> group modes (6 modes):** There are six modes of vibrations due to the NO<sub>2</sub> group, namely, asymmetric NO<sub>2</sub> stretching - $v_{as}(NO_2)$ , symmetric NO<sub>2</sub> stretching- $v_s(NO_2)$ , NO<sub>2</sub> rocking- $\rho(NO_2)$ , NO<sub>2</sub> wagging- $\omega(NO_2)$ , NO<sub>2</sub> scissoring - $\delta(NO_2)$  and NO<sub>2</sub> torsion- $\tau(NO_2)$  which correspond to the frequencies 1511(v<sub>8</sub>), 1226(v<sub>14</sub>), 542(v<sub>31</sub>), 683(v<sub>27</sub>), 819(v<sub>24</sub>) and 74(v<sub>39</sub>) respectively. The NO<sub>2</sub> torsion- $\tau(NO_2)$  is slightly coupled with  $\tau(C_3-O_{11})$  and the other five modes strongly coupled with various vibrational modes. The modes  $v_{as}(NO_2)$ ,

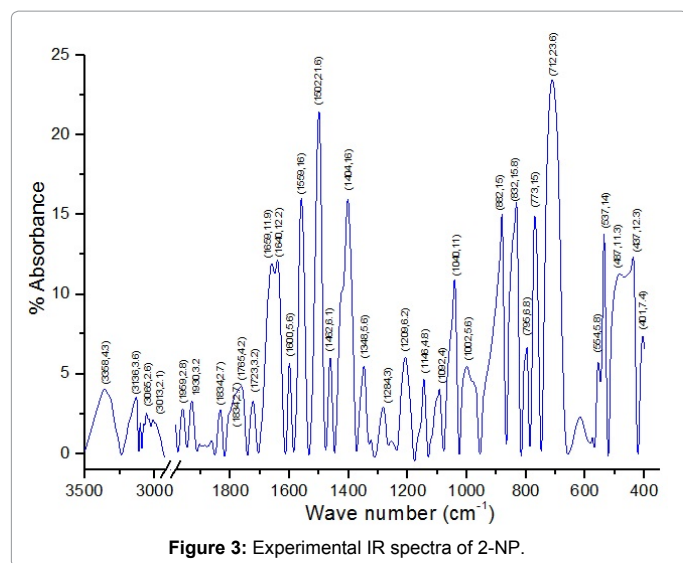


Figure 3: Experimental IR spectra of 2-NP.

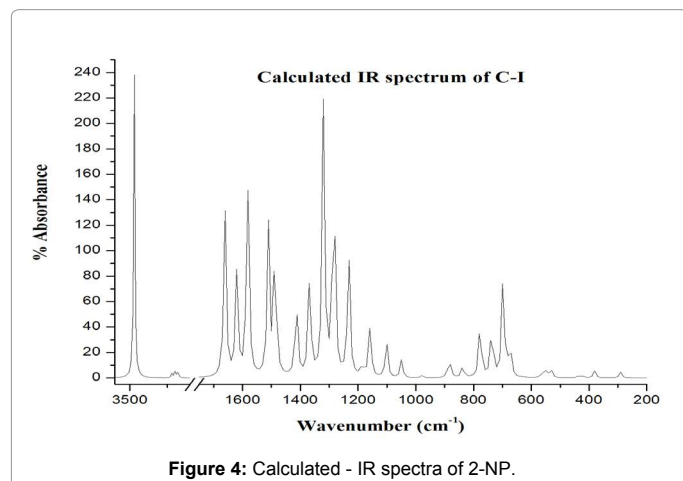


Figure 4: Calculated - IR spectra of 2-NP.

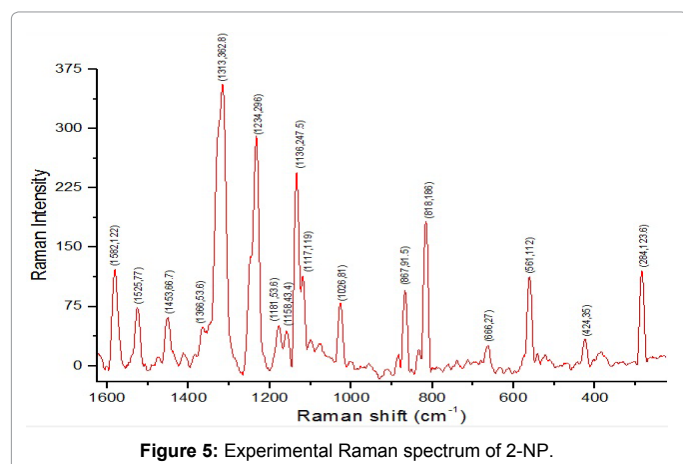


Figure 5: Experimental Raman spectrum of 2-NP.

$\nu_s(\text{NO}_2)$ ,  $\omega(\text{NO}_2)$ ,  $\delta(\text{NO}_2)$  and  $\tau(\text{NO}_2)$  were found to correspond to the frequencies 1560, 1294, 741, 818 and 75  $\text{cm}^{-1}$  [41] and also 1531, 1258, 702, 825 and 165 and also  $\rho(\text{NO}_2)$  corresponds to the frequency 505  $\text{cm}^{-1}$  [48].

#### Comparative study of vibrational modes for the three

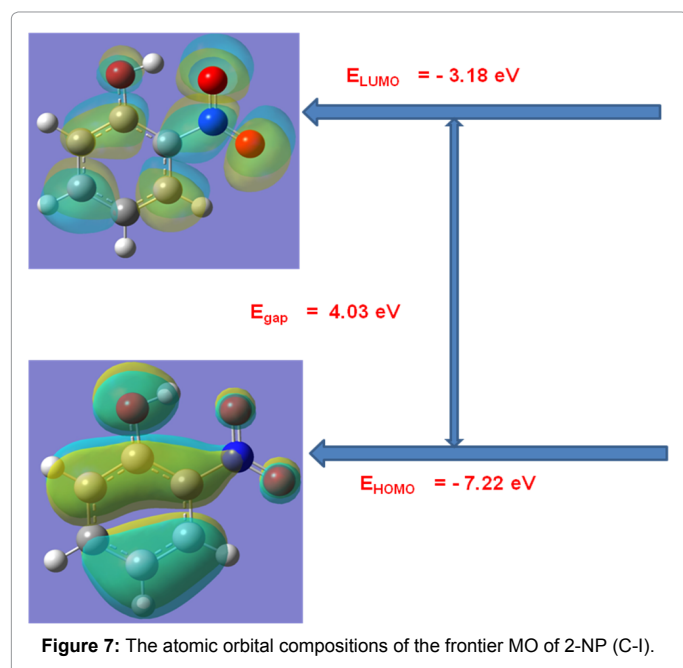
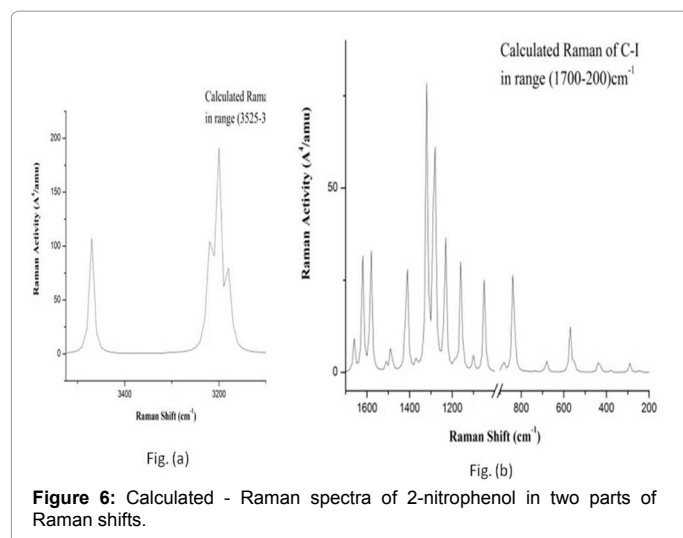
**conformers:** The computed vibrational fundamentals of the three conformers of 2-NP together with their respective differences have been collected in Supplementary material (Table-S1). It could be seen that the modes  $\tau(\text{C-OH})$  and  $\nu(\text{O-H})$  of the OH group show very large frequency differences (in the range 350-400  $\text{cm}^{-1}$ ). Also, the modes  $\tau(\text{C}_4\text{-N}_{13})$ ,  $\beta(\text{C}_3\text{-O}_{11})$ ,  $\omega(\text{NO}_2)$ ,  $\alpha(\text{C}_3\text{-O}_{11}\text{-H}_{12})$  and  $\nu_{\text{as}}(\text{NO}_2)$  show frequency differences of the order of a few tens of a wave number. Clearly, major contribution for this frequency difference is expected to come from H bonding between  $\text{H}_{12}$  and  $\text{O}_{15}$  atoms in the conformer C-1 which is absent in the conformers C-2 /C-3. The phenyl ring modes  $\Phi_3(\text{R})$ ,  $\alpha_3(\text{R})$ ,  $\Phi_2(\text{R})$ ,  $\gamma(\text{C-H})$  and  $\nu(\text{C-H})$  in the C-1 conformer have higher magnitudes than the corresponding modes in the conformers C-2 / C-3. However, the modes  $\omega(\text{NO}_2)$ ,  $\beta(\text{C}_3\text{-O}_{11})$ ,  $\nu(\text{O}_{11}\text{-H}_{12})$ ,  $\Phi_1(\text{R})$ ,  $\nu(\text{C}_3\text{-O}_{11})$ ,  $\nu(\text{R})$  and  $\beta(\text{C}_2\text{-H}_8)$  have higher frequencies in the conformers C-2 /C-3 than their corresponding modes in the most stable one.

The IR intensities and Raman activities for each of the three conformers are collected in Supplementary material (Table-S2). It is noticeable that the IR intensities for the C-1 conformer are much higher than those of the C-2/C-3 conformers for the modes  $\nu(\text{O}_{11}\text{-H}_{12})$ ,  $\nu(\text{C}_3\text{-O}_{11})$ ,  $\nu_s(\text{NO}_2)$ ,  $\beta(\text{C}_2\text{-H}_8)$ ,  $\beta(\text{C}_1\text{-H}_7)$ ,  $\nu(\text{R})$ ,  $\omega(\text{NO}_2)$ ,  $\rho(\text{NO}_2)$  and  $\beta(\text{C}_4\text{-N}_{13})$  ( $\text{S}_2$ ).

The IR intensities for the modes  $\alpha(\text{C}_3\text{-O}_{11}\text{-H}_{12})$ ,  $\nu_{\text{as}}(\text{N}_{13}\text{-O}_{14})$ ,  $\tau(\text{C}_3\text{-O}_{11})$ ,  $\alpha_1(\text{R})$ ,  $\nu(\text{C}_2\text{-H}_8)$ ,  $\nu(\text{C}_5\text{-H}_9)$ ,  $\nu(\text{O}_{11}\text{-H}_{12})$ ,  $\nu_s(\text{NO}_2)$ ,  $\alpha_2(\text{R})$ ,  $\gamma(\text{C}_6\text{-H}_{10})$ ,  $\beta(\text{C}_2\text{-H}_8)$ ,  $\beta(\text{C}_5\text{-H}_9)$ ,  $\delta(\text{NO}_2)$ ,  $\beta(\text{C}_3\text{-O}_{11})$ ,  $\nu(\text{C}_1\text{-H}_7)$  and  $\gamma(\text{C}_4\text{-N}_{13})$  for the conformers C-2/C-3 are much higher than the conformer C-1. One could see the major differences in the Raman activities for the modes  $\nu_s(\text{NO}_2)$ ,  $\nu(\text{C}_3\text{-O}_{11})$ ,  $\alpha(\text{C}_3\text{-O}_{11}\text{-H}_{12})$ ,  $\nu(\text{C}_2\text{-H}_8)$ ,  $\nu(\text{R})$ ,  $\nu(\text{C}_5\text{-H}_9)$ ,  $\alpha_s(\text{NO}_2)$ ,  $\nu(\text{O}_{11}\text{-H}_{12})$ ,  $\nu(\text{C}_1\text{-H}_7)$ ,  $\delta(\text{NO}_2)$ ,  $\beta(\text{C}_1\text{-H}_7)$ ,  $\beta(\text{C}_6\text{-H}_{10})$ ,  $\nu(\text{C}_6\text{-H}_{10})$ , and  $\beta(\text{C}_4\text{-N}_{13})$ . Such discrepancies could be due to the hydrogen bonding in the conformer C-1 and the non-planar geometry of the C-2/C-3 conformers of 2-NP. The highest IR intensity and Raman activity for C-1 occur for the modes  $\nu(\text{O}_{11}\text{-H}_{12})$  and  $\nu(\text{C}_2\text{-H}_8)$  respectively and those for C-2/C-3 for  $\nu_s(\text{NO}_2)$  and  $\nu(\text{C}_2\text{-H}_8)$  respectively. From the above discussion it is clear that the intra-molecular H-bonding plays a crucial role in the molecular conformation.

#### HOMO-LUMO energy gap

The HOMO and LUMO studies are very important for quantum chemistry. These orbitals are also known by the name frontier orbitals, because they lie at the outermost boundaries of the electrons of the molecules. Both the HOMO and the LUMO are the main orbitals that take part in the chemical stability [49]. The kinetic stability of the molecule is measured in terms of energy gap DE [32,50] and the difference of the energies of the HOMO and LUMO is a measure of the excitability of the molecule, the smaller the energy, more easily it can be excited and vice versa. The lower HOMO and LUMO energy gap explains the eventual CT interaction taking place within the molecule, which is responsible for the bioactivity of the molecule. The larger the value of the energy gap the higher the kinetic stability and lower the chemical reactivity because it is energetically unfavorable to add electrons to a high lying LUMO, to remove electrons from a low lying HOMO and so to form the activated complex of any potential reaction [33]. The sketch of the atomic orbital compositions of the frontier MOs are shown in Figure 7. The green and red solid regions in Figure 7 represent the MOs with completely opposite phases. The present calculations predict that the energy gap (DE) of the 2-NP, i.e. the transition energy from HOMO to LUMO of the 2-NP is 0.148189 a.u. This electronic transition corresponds to the transition from the ground to the first excited state and is mainly described by an electron excitation from HOMO to LUMO.



### Global reactivity descriptors

A molecule having high ionization potential ( $V_p$ ) or electron affinity ( $V_A$ ) loses or admits electron hardly [51,52]. By Koopmans' approximation [53,54], the ionization potential and electron affinity of any molecule can be calculated using the relations,

$$V_p = -E_{HOMO}$$

$$V_A = -E_{LUMO}$$

Koopmans' theorem for closed-shell molecules [54] results in the hardness of the molecule;

$$\eta = (V_p - V_A) / 2$$

The chemical potential of the molecule;

$$\mu = -(V_p + V_A) / 2$$

The softness of the molecule;

$$S = 1 / 2\eta$$

The electro negativity of the molecule;

$$\chi = (V_p + V_A) / 2$$

The electro-philicity index of the molecule;

$$\omega = \mu^2 S$$

Using the above relations we find the electro molecular characteristics for 2-NP has been presented in Table-5.

### NLO characteristics: Static polarizability and first order hyperpolarizability

Quantum chemical computational theory has been shown to be essential in the description of the relationship between the electronic structure of the systems and its NLO response [55]. The NLO activities provide the key functions for frequency shifting, optical switching, optical modulation and optical logic to develop the technologies for the communication, signal processing and optical interconnections [56]. The electric dipole moment ( $\mu$ ), the polarizability ( $\alpha$ ) and the hyper polarizability ( $\beta$ ) of the 2-NP molecule have been calculated by finite field method using DFT-B3LYP method employing 6-311++G(d,p) basis set for the isolated molecule, the origin of the Cartesian coordinate system ( $x, y, z$ ) = (0, 0, 0) was chosen at own centre of mass of 2-NP. In the presence of an external electric field, the energy of a system is a function of the field and the first hyperpolarizability is a third rank tensor that can be described by a 3x3x3 matrix. The 27 components of the 3D matrix can be reduced to 10 components using the Klein man symmetry [57]. The matrix can be given in the lower tetrahedral format. Clearly, the lower part of the 3x3x3 matrices is a tetrahedral. The components of  $\beta$  are defined as the coefficients in the Taylor series expansion of the energy in the external electric field. If the external field is weak and homogeneous, this expansion is as given below,

$$E = E^0 - \mu_i F_i - 1/2(\alpha_{ij} F_i F_j - 1/6(\beta_{ijk} F_i F_j F_k) + \dots$$

Here,  $E^0$  is the energy of the unperturbed molecules,  $F_i$  is the field at the origin,  $\mu_i$ ,  $\alpha_{ij}$  and  $\beta_{ijk}$  are the components of dipole moment, polarizability and first hyperpolarizability, respectively.

The total static dipole moment  $\mu$ , the mean polarizability  $\alpha_0$ , the anisotropy of the polarizability  $\Delta\alpha$  and the mean first hyperpolarizability  $\beta_0$ , using the x, y and z components are defined as;

Dipole moment;

$$\mu = (\mu_x^2 + \mu_y^2 + \mu_z^2)^{1/2}$$

Static polarizability;

$$\alpha_0 \alpha_0 = (\alpha_{xx} + \alpha_{yy} + \alpha_{zz}) / 3$$

The total polarizability;

$$\Delta\alpha = (1/\sqrt{2})\sqrt{[(\alpha_{xx} - \alpha_{yy})^2 + (\alpha_{yy} - \alpha_{zz})^2 + (\alpha_{zz} - \alpha_{xx})^2 + 6\{\alpha_{xy}^2 + \alpha_{yz}^2 + \alpha_{zx}^2\}]}$$

First order hyperpolarizability;

$$\beta_0 = \sqrt{[\sum \beta_x^2]}$$

Where

$$\beta_x = (\beta_{xxx} + \beta_{xyy} + \beta_{xzz})$$

$$\beta_y = (\beta_{yxx} + \beta_{yyy} + \beta_{yzz})$$

$$\beta_z = (\beta_{zxx} + \beta_{zyy} + \beta_{zzz})$$

The static polarizability  $\alpha_0$  (91.966 au) and total polarizability  $\Delta\alpha$  (9483.787 au) of the 2-NP together with all its components and perturbation to all its components, first order hyperpolarizability ( $\beta = 426.118$  au) and its components and the total as well as components of the dipole moment have been tabulated in the Table-5.

### Electrostatic potential

The electrostatic potential (ESP) is the tool which is used to study the intermolecular association and molecular properties of small molecules, actions of drug molecules and their analogues, the biological function of haemoglobin and enzyme catalysis [33,58-61]. ESP is widely used as the reactivity map displaying most probable regions for the electrophilic attack of charged point-like reagents on organic molecules [62]. The values and spatial distribution of ESP are in fact responsible for the chemical behaviour of an agent in a chemical reaction. They strongly influence the binding of a substrate to its active site. ESP is typically visualized through mapping its values onto the molecular ED. The different values of the electrostatic potential at the surface are represented by different colors; the red represents regions of the most negative electrostatic potential, the blue represents regions of the most positive electrostatic potential and the green represents regions of zero potential. Potential increases in the order red, orange, yellow, green and blue. While the negative electrostatic potential corresponds to an attraction of the proton by the concentrated ED in the molecule (and is colored in shades of red), the positive electrostatic potential corresponds to the repulsion of the proton by atomic nuclei in regions where a low ED exists and the nuclear charge is incompletely shielded (and is colored in shades of blue). The total density plot and its array of the 2-NP are shown in the Figure 8. The molecular ESP values, corresponding to Merge-Singh-Koll man scheme [47], of the 2-NP molecule have been arranged in the Table 3. Also, the diagrammatic demonstration of the MESP via map and its contour has been shown in Figure 9. These Figs provide a visual representation of the chemically active sites and comparative reactivity of atoms. The ESP plots and the value arranged in the Table 3 predict that there are no regions of positive and zero potential present in the molecule. Also, the Figure 9 and the data in the Table 3 predict that the sites associated with the functional groups, namely, OH and NO<sub>2</sub> groups are most reactive sites for the nucleophilic reactions.

### Thermo molecular characteristics

The studies of some thermo molecular characteristics, namely, zero point vibrational energy, enthalpy, Gibb's free energy, internal energy, entropy, heat capacity, thermal energy and the partition functions etc. have been found to play crucial role in the material characterization. We have presented some thermal parameters in Table 6. It can be noticed that all of the analysed thermodynamic parameters are increasing with the temperature but G is found to decrease with T [Figure 10(a)-10(h)] while the zero point vibrational energy remains constant (67.226 Kcal/mol) at all the temperature because it is a characteristic property of the molecule. All the fitting parameters and other essential statistical data have been demonstrated together with the fitted graphs of these parameters. All of the characteristic thermal properties of crystalline 2-NP solid have been found to be in agreement with the explanation of Dulong-Pettit law as well as of Einstein's thermo dynamical theory of crystalline solids. The fitting equations of the thermal parameters of 2-NP are as given below;

$$[\text{Log}_e q(t, e, r, v)]_{\text{Ref. - 1st Vib state}} = 51.2676 - 837.243 \exp\left(-\frac{T}{43.5306}\right) - 311.0166 \exp\left(-\frac{T}{124.5469}\right) - 162.7858 \exp\left(-\frac{T}{622.2405}\right)$$

$$(R^2 = 1, \chi^2 = 1.7599 \times 10^{-5})$$

$$[\text{Log}_e q(t, e, r, v)]_{\text{Ref. - 1st Vib state}} = 23.9202 + (0.0388) T - (11.04) T^2 \quad (R^2 = 0.999)$$

$$S_{m^0} = 52.5299 + (0.1240) T - (2.8791 \times 10^{-5}) T^2 \quad (R^2 = 0.99999)$$

$$c_{p,m^0} = -0.9985 + (0.1195) T - (5.4209) T^2 \quad (R^2 = 0.999)$$

$$H_{m^0} = 66.321 + (0.0120) T + (3.3350) T^2 \quad (R^2 = 0.9993)$$

$$U_{m^0} = 65.7785 + (0.0120) T + (3.3350) T^2 \quad (R^2 = 0.9993)$$

$$Q_{m^0} = 66.3222 + (0.0100) T + (0.3335) T^2 \quad (R^2 = 0.9993)$$

$$G_{m^0} = 68.2813 - (0.0586) T - (4.7655) T^2 \quad (R^2 = 0.9999)$$

All the thermo molecular data provide the crucial and helpful information for the further study on the 2-NP. They can be applied to compute the other thermodynamic characteristics according to relationships of thermo dynamical parameters and estimate directions of chemical reactions according to the second law of thermodynamics in thermo chemical fields. It should be noticeable that all calculations of thermo dynamical parameters have been done in gas phase and they could not be used in solution phase.

### NMR characterization: Magnetic susceptibility, shielding and current density tensors

The NMR analysis plays an essential part in material characterization in presence of magnetic fields. This type investigation provides chemical shifts and magnetic shielding tensors to each atomic site of the molecule as well as magnetic susceptibility and the current density tensor for the material being investigated. We have applied Continuous Set Gauge of Transformation (CSGT) method for NMR investigation of the 2-NP molecule. The magnetic susceptibility tensor of 2-NP has been computed as

$$X_{ij} = \begin{bmatrix} -41.82 & -3.21 & -0.01 \\ -3.06 & -40.23 & 0.01 \\ -0.01 & 0.01 & -111.72 \end{bmatrix}$$

Having the Eigen values  $\lambda_1 = -111.7209$ ,  $\lambda_2 = -44.2576$  and  $\lambda_3 = -37.7896$  and the value of magnetic susceptibility  $\chi$  is found to be -64.5893 cgs-ppm, the negative sign of  $\chi$  shows the diamagnetic nature of the 2-NP molecule.

Also, the magnetic shielding tensors together with their corresponding Eigen values at different atomic sites computed are depicted as below;

$$C_1 : \sigma_{ij}^{c_1} = \begin{bmatrix} -71.44 & 8.10 & 0.11 \\ 9.44 & 23.35 & -0.04 \\ 0.09 & -0.04 & 169.96 \end{bmatrix} \quad C_2 : \sigma_{ij}^{c_2} = \begin{bmatrix} 29.73 & 29.20 & 0.06 \\ 33.52 & -9.23 & -0.06 \\ 0.08 & -0.03 & 158.67 \end{bmatrix}$$

$$\lambda_1 = -72.25, \lambda_2 = 24.16 \text{ and } \lambda_3 = 169.9 \quad \lambda_1 = -26.67, \lambda_2 = 47.17 \text{ and } \lambda_3 = 158.67$$

$$C_3 : \sigma_{ij}^{c_3} = \begin{bmatrix} -21.45 & -23.40 & 0.04 \\ 3.26 & -37.00 & 0.01 \\ -0.02 & 0.04 & 119.98 \end{bmatrix} \quad C_4 : \sigma_{ij}^{c_4} = \begin{bmatrix} 3.97 & 14.74 & -0.02 \\ -7.92 & 16.60 & -0.02 \\ 0.09 & 0.01 & 117.78 \end{bmatrix}$$

$$\lambda_1 = -41.94, \lambda_2 = -16.50 \text{ and } \lambda_3 = 119.98 \quad \lambda_1 = 3.11, \lambda_2 = 17.46 \text{ and } \lambda_3 = 117.78$$

$$C_5 : \sigma_{ij}^{c_5} = \begin{bmatrix} 21.47 & 31.27 & 0.03 \\ 12.38 & -31.99 & -0.02 \\ 0.05 & 0.00 & 172.29 \end{bmatrix} \quad C_6 : \sigma_{ij}^{c_6} = \begin{bmatrix} 26.49 & -35.07 & 0.02 \\ -39.51 & -16.53 & -0.04 \\ 0.04 & -0.01 & 172.56 \end{bmatrix}$$

$$\lambda_1 = -39.76, \lambda_2 = 29.24 \text{ and } \lambda_3 = 172.29 \quad \lambda_1 = -38.07, \lambda_2 = 48.03 \text{ and } \lambda_3 = 172.56$$

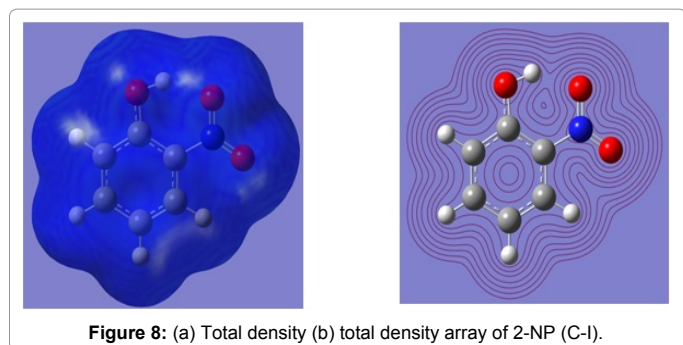


Figure 8: (a) Total density (b) total density array of 2-NP (C-I).

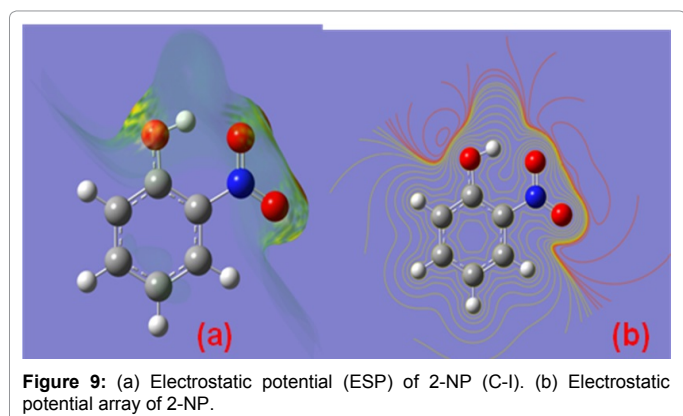


Figure 9: (a) Electrostatic potential (ESP) of 2-NP (C-I). (b) Electrostatic potential array of 2-NP.

$$H_7 : \sigma_{ij}^{C_1} = \begin{bmatrix} 22.75 & 0.52 & 0 \\ 0.74 & 24.26 & 0 \\ -0.002 & 0 & 21.83 \end{bmatrix} \quad H_8 : \sigma_{ij}^{H_8} = \begin{bmatrix} 27.52 & 1.41 & -0.001 \\ 2.28 & 24.35 & -0.002 \\ -0.004 & 0.002 & 21.37 \end{bmatrix}$$

$$\lambda_1 = 21.83, \lambda_2 = 22.70 \text{ and } \lambda_3 = 27.88 \quad \lambda_1 = 21.37, \lambda_2 = 23.50 \text{ and } \lambda_3 = 28.37$$

$$H_9 : \sigma_{ij}^{H_9} = \begin{bmatrix} 26.74 & 1.36 & 0 \\ 0.74 & 24.26 & 0 \\ -0.001 & -0.003 & 20.34 \end{bmatrix} \quad H_{10} : \sigma_{ij}^{H_{10}} = \begin{bmatrix} 27.07 & -1.38 & -0.002 \\ -1.59 & 25.46 & 0 \\ -0.0004 & 0.003 & 22.21 \end{bmatrix}$$

$$\lambda_1 = 20.34, \lambda_2 = 23.87 \text{ and } \lambda_3 = 27.12 \quad \lambda_1 = 22.21, \lambda_2 = 24.58 \text{ and } \lambda_3 = 27.96$$

$$O_{11} : \sigma_{ij}^{O_{11}} = \begin{bmatrix} 98.07 & -1.38 & -0.002 \\ 9.71 & 161.51 & -0.002 \\ 0.16 & 0.12 & 286.79 \end{bmatrix} \quad H_{12} : \sigma_{ij}^{H_{12}} = \begin{bmatrix} 33.34 & -1.38 & -0.002 \\ -1.08 & 20.94 & -0.001 \\ 0.02 & -0.06 & 10.39 \end{bmatrix}$$

$$\lambda_1 = 85.06, \lambda_2 = 174.53 \text{ and } \lambda_3 = 286.79 \quad \lambda_1 = 10.39, \lambda_2 = 20.50 \text{ and } \lambda_3 = 33.78$$

$$N_{13} : \sigma_{ij}^{N_{13}} = \begin{bmatrix} -274.04 & -14.18 & -0.16 \\ -7.61 & -209.55 & -0.04 \\ -0.13 & -0.04 & 41.91 \end{bmatrix} \quad O_{14} : \sigma_{ij}^{O_{14}} = \begin{bmatrix} -450.67 & 153.53 & -0.28 \\ -0.51 & -682.72 & -0.09 \\ -0.31 & 0.08 & 154.15 \end{bmatrix}$$

$$\lambda_1 = -275.83, \lambda_2 = -207.76 \text{ and } \lambda_3 = 41.91 \quad \lambda_1 = -705.68, \lambda_2 = -427.72 \text{ and } \lambda_3 = 154.15$$

$$O_{15} : \sigma_{ij}^{O_{15}} = \begin{bmatrix} -398.51 & -79.71 & -0.27 \\ 128.83 & -506.31 & 0.01 \\ -0.17 & -0.04 & 113.76 \end{bmatrix}$$

$$\lambda_1 = -511.64, \lambda_2 = -393.18 \text{ and } \lambda_3 = 113.76$$

The magnetic shielding at the atomic sites, namely, C<sub>1</sub>, C<sub>2</sub>, C<sub>3</sub>, C<sub>4</sub>, C<sub>5</sub>, C<sub>6</sub>, H<sub>7</sub>, H<sub>8</sub>, H<sub>9</sub>, H<sub>10</sub>, O<sub>11</sub>, H<sub>12</sub>, N<sub>13</sub>, O<sub>14</sub> and O<sub>15</sub> have been computed 40.625, 59.723, 20.510, 46.115, 53.924, 60.840, 24.138, 24.414, 23.778, 20.340, 182.124, 21.558, -147.229, -326.418 and -263.685 ppm, respectively. It is noticeable that the shielding at every sites associated to NO<sub>2</sub> group is negative and attaining higher values [Figure 11(a, b)]. From the Figure 11 it is obvious that the effect of the magnetic field is least nearby the NO<sub>2</sub> group of 2-NP molecule.

The current density tensor (J) for the 2-NP have been computed and depicted in matrix form as;

$$J_{ij} = \begin{bmatrix} 0.0002 & 0.0001 & 0.0139 \\ 0.0004 & 0 & 0.3173 \\ 0.0084 & -0.2080 & 0.0001 \end{bmatrix}$$

The two Eigen values of the current density tensor have been found imaginary while one Eigen value of J is  $\lambda=0.0002$  for 2-NP molecule. The value of the J ( $\sim 1.231 \times 10^{-5}$  a.u.) has been found to be negligibly small, which reveals that the electrical conductivity of 2-NP molecule is negligibly small. The mapping and corresponding contour of J for the title molecule have been demonstrated diagrammatically (Figure 12). Figure 12 also represents that the current density is extremely weak for the 2-NP molecule.

## Conclusions

For the first time; complete material characterization, complete vibrational mode assignment, conformational analysis, HOMO – LUMO analysis, complete data analysis on thermo-dynamical parameters, data analysis on reactivity parameters and on NMR parameters, potential energy distribution and investigations of APT, Mulliken atomic charges and ESP derived charge of 2-NP has been carried out. The 2-NP molecule has been expected to possess three conformations out of which lowest energy conformer is planar possessing C<sub>s</sub> symmetry while other two are non-planar possessing

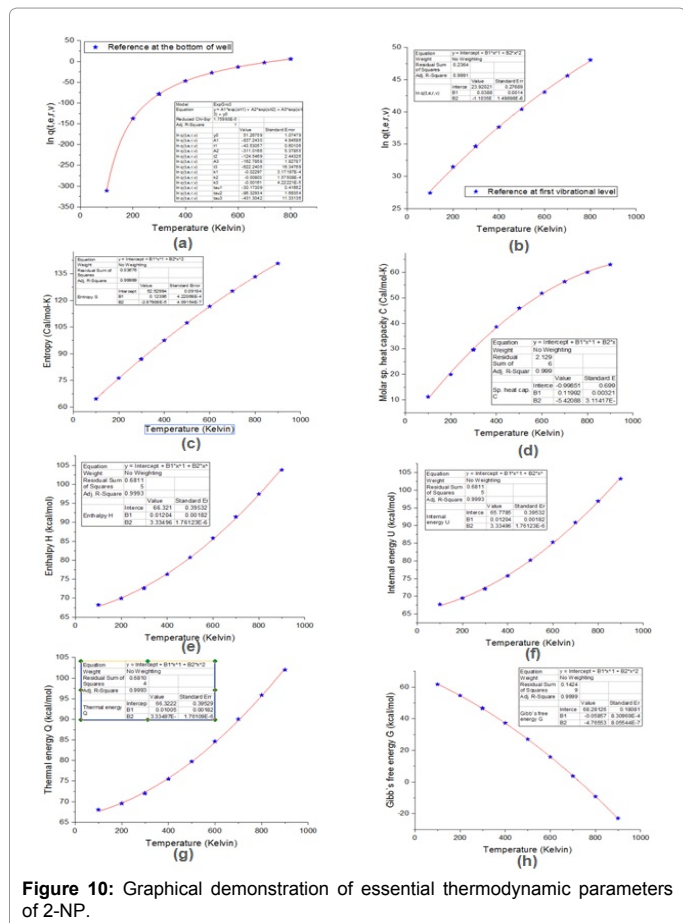


Figure 10: Graphical demonstration of essential thermodynamic parameters of 2-NP.

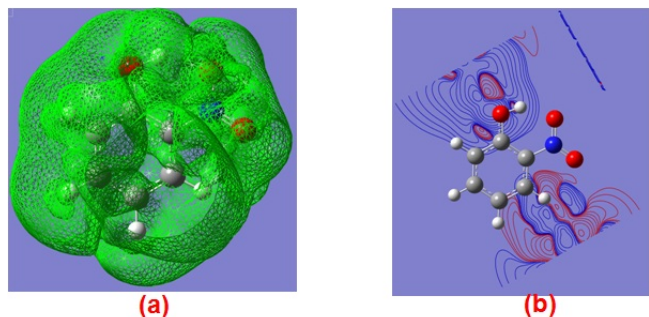


Figure 11: Map (left) and contour (right) of magnetic shielding on 2-NP.

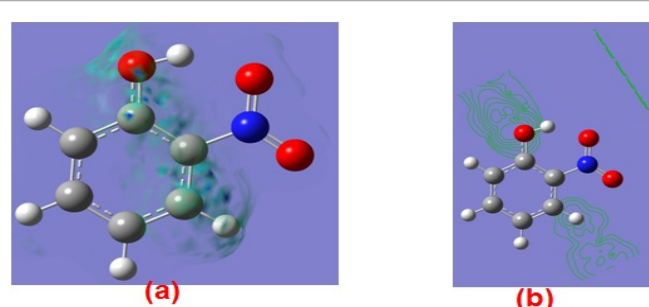


Figure 12: Current density demonstration through map (left) and contour (right) for 2-NP.

$C_1$  symmetry. Conformer C-1 is planar, in which  $\text{NO}_2$  group is in the plane of phenyl ring while in conformers C-2 and C-3 the plane of  $\text{NO}_2$  group makes the angle  $-33.7^\circ$  and  $33.7^\circ$  respectively. The Nitrogen atom of  $\text{NO}_2$  group attains highest APT charge while carbon atom directly attached to OH group bears highest Mulliken charge. For lowest energy conformer  $\alpha$  ( $C_4-C_3-O_{11}$ ) is largest ( $124.6^\circ$ ) and  $\alpha(C_3-O_{11}-H_{12})$  is smallest ( $107.3^\circ$ ) respectively. For the modes  $\tau(C_3-O_{11})$  and  $\nu(O_{11}-H_{12})$  are found to have very large frequency differences  $394$  and  $-352 \text{ cm}^{-1}$  respectively among the conformers C-1 and C-2/C-2.  $\nu(O_{11}-H_{12})$  is of largest IR intensity and  $\nu(C_2-H_8)$  is found to be largest Raman activity mode. All the modes of vibrations are precisely assigned to the corresponding appropriate frequencies and also the experimental work has been compared with the computational work as well as the work already been carried out, which found to be in agreement with our work. The HOMO-LUMO transition clearly explicates CT interaction involving donor and acceptor groups. The ESP plots and corresponding values show that there are nucleophilic most reactive regions are found nearby OH and  $\text{NO}_2$  groups while no regions of positive and zero potential present in the molecule. The HOMO - LUMO energy gap is found to be  $\Delta E = 0.148189 \text{ a.u.}$  In conformer C-1 intramolecular hydrogen bonding  $O_{15} \cdots H_{12}$  is expected in 2-NP molecule. NMR investigations as well as HOMO- LUMO theory reveal that the conductivity of the title molecule is extremely low and the molecule is diamagnetic in nature.

Reactivity Descriptor		Dipole Moment( $\mu$ )		Polarizability ( $\alpha$ )					1 <sup>st</sup> order Hyperpolarizability( $\beta$ )		
				Para.	Exact		Perturbation to $\alpha$		Para.	a.u.	esu *10 <sup>-32</sup>
Para.	Value	Para.	Debye		(a.u.)	esu *10 <sup>-24</sup>	(a.u.)	esu *10 <sup>-24</sup>			
$V_p$	6.635	( $\mu_{x/FI}$ )	-3.951	$\alpha_{xx}$	123.434	18.268	74.308	10.998	$\beta_{xxx}$	524.773	4534.563
$V_A$	0.881	( $\mu_{y/FI}$ )	-0.611	$\alpha_{xy}$	-0.198	-0.029	-1.208	-0.179	$\beta_{xxy}$	-125.223	-581.160
$\eta$	2.877	( $\mu_{z/FI}$ )	-0.001	$\alpha_{yy}$	105.178	15.566	95.758	14.172	$\beta_{xyy}$	-102.311	-884.069
$\mu$	-3.758	( $\mu_{FI}$ )	3.998	$\alpha_{xz}$	-0.005	-0.001	-0.002	-0.0003	$\beta_{yyy}$	-95.389	-824.256
S	0.174	( $\mu_{x/esp}$ )	-3.964	$\alpha_{yz}$	0.012	0.002	0.023	0.003	$\beta_{xzx}$	-0.080	-0.691
$\chi$	3.758	( $\mu_{y/esp}$ )	-0.603	$\alpha_{zz}$	47.285	6.998	23.282	3.446	$\beta_{yyz}$	-0.023	-0.199
$\omega$	2.457	( $\mu_{z/esp}$ )	-0.003	$\alpha_0$	91.966	13.612	64.449	9.538	$\beta_{yzz}$	-0.014	-0.121
$E_g$	4.03	( $\mu_{esp}$ )	4.010	$\Delta\alpha$	9483.787	1403.600	8325.284	1232.142	$\beta_{zzz}$	-75.942	-656.215
									$\beta_{zzz}$	-27.380	-236.590
									$\beta_{zzz}$	-0.013	-0.112
									$\beta_{total}$	426.118	3681.229

\*  $V_p$  = Ionization potential,  $V_A$  = Electron affinity,  $\eta$  = Hardness,  $\mu$  = Chemical potential, S = Softness,  $\chi$  = Electro-negativity,  $\omega$  = electro-philicity of the molecules.

Table 5: Molecular reactivity and NLO parameters of C-1 conformer of 2-NP.

T (K)	G Kcal/mol	H Kcal/mol	Q Kcal/mol	C cal/mol-K	S cal/mol-K	U Kcal/mol	ZPE Kcal/mol	$\text{Ln}Q_{v=0}$	$\text{Ln}Q_{\text{Bot}}$
100	61.7744	68.2344	68.037	11.236	64.604	67.6919	67.226	27.427241	-310.866945
200	54.7113	69.9739	69.578	19.973	76.312	69.4314	67.226	31.484367	-137.662726
298.15	46.7007	72.6006	72.010	29.552	86.870	72.0581	67.226	34.641248	-78.823178
300	46.5394	72.6589	72.064	29.728	87.066	72.1164	67.226	34.697505	-78.067224
400	37.3109	76.2864	75.493	38.613	97.440	75.7439	67.226	37.633424	-46.940123
500	27.0689	80.7254	79.734	45.928	107.316	80.1829	67.226	40.415236	-27.243602
600	15.8687	85.8181	84.628	51.726	116.585	85.2756	67.226	43.073074	-13.309290
700	3.7721	91.4280	90.039	56.315	125.223	90.8855	67.226	45.615146	-2.712595
800	-9.1554	97.4488	95.861	60.001	133.258	96.9063	67.226	48.045839	5.759065
900	-22.8595	103.8028	102.017	63.013	140.739	103.2603	67.226		

\* T = Temperature, G = Gibb's free energy, H = Enthalpy, Q = Thermal energy, C = Molar heat capacity, S = Entropy, U = Internal energy, ZPE = Zero point vibrational energy,  $Q_{v=0}$  = Total partition function taking reference 1<sup>st</sup> vibrational level,  $Q_{\text{Bot}}$  = Total partition function taking reference at bottom of the well.

Table 6: Some crucial molecular thermodynamic parameters of C-1 conformer of 2-NP.

## Reference

1. Leuenberger C, Ligocki MP, Pankow JF (1985) Trace organic compounds in rain. 4. Identities, concentrations, and scavenging mechanisms for phenols in urban air and rain. *Environ Sci Technol* 19: 1053-1058.
2. Tremp J, Mattrel P, Fingler S, Giger W (1993) Phenols and Nitrophenols as tropospheric pollutants: emissions from automobile exhausts and phase transfer in the atmosphere. *Water Air Soil Pollut.* 68: 113-123.
3. Luttko J, Levsen K (1997) Phase Partitioning of Phenol and Nitrophenols in clouds. *Atmos. Environ.* 31: 2649-2655.
4. Zhang DP, Wu WL, Long HY, Liu YC, Yang ZS (2008) Voltammetric Behavior of o-Nitrophenol and Damage to DNA. *Int J Mol Sci* 9: 316-326.
5. Pedrosa VA, Codognoto L, Avaca LA (2003) Electroanalytical Determination of 4-Nitrophenol by Square Wave Voltammetry on Diamond Electrodes. *J. Braz. Chem. Soc.* 14: 530-536.
6. Uberoi V, Bhattacharya SK (1997) Toxicity and degradability of nitrophenols in anaerobic systems. *Water. Environ. Res.* 69: 146-156.
7. Zaggout FR, Abu Ghalwa N (2008) Removal of o-nitrophenol from water by electrochemical degradation using a lead oxide/titanium modified electrode. *J Environ Manage* 86: 291-296.
8. Canizares P, Lobato J, Paz R, Rodrigo MA, Sáez C (2005) Electrochemical oxidation of phenolic wastes with boron-doped diamond anodes. *Water Res* 39: 2687-2703.
9. Qin Y, Wheeler RA (1996) Density-Functional-Derived Structures, Spin Properties, and Vibrations for Phenol Radical Cation. *J. Phys. Chem.* 100: 10554-10563.
10. Lampert H, Mikenda W, Karpfen A (1996) Intramolecular Hydrogen Bonding in 2-Hydroxybenzoyl Compounds: Infrared Spectra and Quantum Chemical Calculations. *J. Phys. Chem.* 100: 7418-7425.
11. De Heer MI, Korth HG, Mulder P (1999) Poly Methoxy Phenols in Solution: OH Bond Dissociation Enthalpies, Structures, and Hydrogen Bonding. *J. Org. Chem.* 64: 6969-6975.
12. De Heer MI, Mulder P, Korth HG, Ingold K, Luszyk J (2000) Hydrogen Atom Abstraction Kinetics from Intramolecularly Hydrogen Bonded Ubiquinol-0 and Other (Poly) methoxy Phenols. *J. Am. Chem. Soc.* 122: 2355-2360.
13. Bene JED, Person WB, Szczepaniak K (1995) Properties of Hydrogen-Bonded Complexes Obtained from the B3LYP Functional with 6-31G (d,p) and 6-31+G (d,p) Basis Sets: Comparison with MP2/6-31+G(d,p) Results and Experimental Data. *J. Phys. Chem.* 99: 10705-10707.
14. Zierkiewicz W, Michalska D, Matuszewicz BC, Raspenk M (2003) Molecular Structure and Infrared Spectra of 4-Fluorophenol: A Combined Theoretical and Spectroscopic Study. *J Phys. Chem. A* 107: 4547-4554.
15. Borisenko KB, Bock CW, Hargittai I (1994) Intramolecular Hydrogen Bonding and Molecular Geometry of 2-Nitrophenol from a Joint Gas-Phase Electron Diffraction and ab Initio Molecular Orbital Investigation. *J. Phys. Chem.* 98: 1442-1448.
16. Kovacs A, Izvekov V, Keresztury G, Pongor G (1998) Vibrational analysis of 2-nitrophenol: A joint FT-IR, FT-Raman and scaled quantum mechanical study. *Chem. Phys.* 238: 231-243.
17. Abkowicz-Bienko AJ, Latajka Z, Bienko D, Michalska D (1999) Theoretical infrared spectrum and revised assignment for para-nitrophenol. Density functional theory studies. *Chem. Phys.* 250: 123-129.
18. Korth HG, de Heer MI, Mulder P (2002) A DFT Study on Intramolecular Hydrogen Bonding in 2-Substituted Phenols: Conformations, Enthalpies, and Correlation with Solute Parameters. *J. Phys. Chem.* 106: 8779-8789.
19. Rauhut G, Pulay P (1995) Transferable Scaling Factors for Density Functional Derived Vibrational Force Fields. *J. Phys. Chem.* 99: 3093-3100.
20. Macsari I, Izvekov V, Kovacs A (1997) Scaled quantum mechanical study of 2,6-difluorophenol: a fluorine-containing weak hydrogen-bonded system. *Chem. Phys. Lett.* 269: 393-400.
21. Behringer J (1958) The connection of Raman dispersion, adsorption and fluorescence (resonance Raman effect). *Z. Elektrochem.* 62: 544-567.
22. Green JHS, Kynaston W, Lindsey AS (1961) The vibrational spectra of benzene derivatives-I Nitrobenzene, the benzose ion, alkali metal benzoates and salicylates. *Spectrochim. Acta* 17: 486-502.
23. Horak M, Smolikova J, Pitha J (1961) Spectroscopic study of the hydrogen bond in substituted 2-nitrophenols. *Coll. Czech. Chem. Commun.* 26: 2891-2896.
24. Robinson EA, Schreiber HD, Spencer JN (1971) Solvent and temperature effects on the hydrogen bond. *J. Phys. Chem.* 75: 2219-2222.
25. Bedarek V, Janu I, Jirkovszky J, Socha J, Klicnar J (1972) Influence of substitution of aromatic nucleus on frequency of valence vibrations of groups bonded by hydrogen bond. *Coll. Czech. Chem. Commun.* 37: 3447-3450.
26. Leavell S, Curl Jr. R (1973) Microwave spectrum of 2-nitrophenol: Structure of the hydrogen bond. *J. Mol. Spectrosc.* 45: 428-442.
27. Kishore Y, Sharma NS, Dwiredi CPD (1974) *Indian J. Phys.* 48 412.
28. Dietrich SW, Jorgensen EC, Kollman PA, Rothenberg S (1976) A theoretical study of intramolecular hydrogen bonding in ortho-substituted phenols and thiophenols. *J. Am. Chem. Soc.* 98: 8310-8324.
29. Canadell E, Catalan J, Fernandez-Alonso JI (1978) *Adv. Mol. Relaxation Interact. Process.* 12 265.
30. Iwasaki F, Kawano Y (1978) The crystal and molecular structure of o-nitrophenol. *Acta Crystallogr.* B34: 1286-1290.
31. Schreiber V, Koll A, Kulbida A, Majerz I (1995) IR matrix isolation and MNDO/PM3 studies of ortho-substituted phenols with intramolecular H-bonds. *J. Mol. Struct.* 348: 365-368.
32. Foresman JB, Frisch AE (1996) *Exploring Chemistry with Electronic Structure Methods*, (2nd ed), Gaussian, Pittsburgh, PA.
33. Manolopoulos DF, May JC, Down SE (1991) Theoretical studies of the fullerenes: C34 to C70 *Chem. Phys. Lett.* 181: 105-111.
34. Seminario JM, Politzer P (1995) *Modern Density Functional Theory: A Tool for Chemistry*, Elsevier, Amsterdam.
35. Becke AD (1993) Density-functional thermochemistry. III. The role of exact exchange. *J. Chem. Phys.* 98: 5648-5652.
36. Becke AD (1988) Density-functional exchange-energy approximation with correct asymptotic behavior. *Phys Rev A* 38: 3098-3100.
37. Lee C, Yang W, Parr RG (1988) Development of the Colle-Salvetti correlation-energy formula into a functional of the electron density. *Phys Rev B Condens Matter* 37: 785-789.
38. Vosko SH, Wilk L, Nusair M (1980) Accurate spin-dependent electron liquid correlation energies for local spin density calculations: a critical analysis. *Can. J. Phys.* 58: 1200-1211.
39. Frisch MJ, Trucks GW, Schlegel HB, Scuseria GE (2010) *Gaussian 09, Revision C.01*, Gaussian, Inc., allingford, CT.
40. Martin JML, Van Alsenoy C (1995) GAR2PED, A Program to Obtain a Potential Energy Distribution from a Gaussian Archive Record, University of Antwerp, Belgium.
41. Ferreira MMC, Suto E (1992) Atomic Polar Tensor Transferability and Atomic Charges for the Fluoro-methane Series CH<sub>x</sub>F<sub>4-x</sub>. *J. Phys. Chem.* 96: 8844-8849.
42. Dixit V, Yadav RA (2015) *Asian J Phys*, 24, in press.
43. Martin F, Zipse H (2005) Charge distribution in the water molecule—a comparison of methods. *J Comput Chem* 26: 97-105.
44. Besler BH, Merz KM, Kollman PA (1990) Atomic charges derived from semi-empirical methods. *J Comput Chem*, 11: 431-439.
45. Sing UC, Kollman PA (1984) An approach to computing electrostatic charges for molecules. *J Comput Chem*, 5: 129-145.
46. Chis V (2004) Molecular and vibrational structure of 2,4-dinitrophenol: FT-IR, FT-Raman and quantum chemical calculations. *Chemical Physics* 300: 1-11.
47. Dixit V, Yadav RA (2015) DFT-B3LYP computations of electro and thermo molecular characteristics and mode of action of fungicides (chlorophenols). *Int J Pharm* 491: 277-284.
48. Lewars E (2003) *Computational Chemistry Introduction to the Theory and Applications of Molecular and Quantum Mechanics*, Kluwer Academic Publishers, Norwell, MA.
49. Chang R (2001) *Chemistry*, (7th ed) McGraw-Hill, New York.

50. Koopmans TA (1934) Über die Zuordnung von Wellenfunktionen und Eigenwerten zu den einzelnen Elektronen eines Atoms. *Physica* 1: 104-113.
51. Govindarasu K, Kavitha E (2014) Molecular structure, vibrational spectra, NBO, UV and first order hyperpolarizability, analysis of 4-Chloro-DL-phenylalanine by density functional theory. *Spectrochimica Acta Part A* 133: 799-810.
52. Burland DM, Miller RD, Walsh CA (1994) Second-order nonlinearity in poled-polymer systems. *Chem. Rev.* 94: 31-75.
53. Geskin VM, Lambert C, Brédas JL (2003) Origin of high second- and third-order nonlinear optical response in ammonio/borato diphenylpolyene zwitterions: the remarkable role of polarized aromatic groups. *J Am Chem Soc* 125: 15651-15658.
54. Kleinman DA (1977) Nonlinear Dielectric Polarization in Optical Media. *Phys. Rev.* 126: 1962-1979.
55. Tomasi J, Politzer P, Truhlar D (Eds.) (1981) *Chemical Application of Atomic and Molecular Electrostatic Potentials*, Plenum, New York 257-294.
56. Moro S, Bacilieri M, Ferrari C, Spalluto G (2005) Autocorrelation of molecular electrostatic potential surface properties combined with partial least squares analysis as alternative attractive tool to generate ligand-based 3D-QSARs. *Curr Drug Discov Technol* 2: 13-21.
57. Murray JS, Sen K (1996) *Molecular Electrostatic Potentials, Concepts and Applications*, Elsevier, Amsterdam.
58. Weiner PK, Langridge R, Blaney JM, Schaefer R, Kollman PA (1982) Electrostatic potential molecular surfaces. *Proc Natl Acad Sci U S A* 79: 3754-3758.
59. Politzer P, Truhlar DG (1981) *Chemical Application of Atomic and Molecular Electrostatic Potentials*, Plenum, New York.
60. JS Murray, K Sen (1996) *Molecular Electrostatic Potentials, Concepts and Applications*, Elsevier, 558 Amsterdam.
61. Weiner PK, Langridge R, Blaney JM, Schaefer R, Kollman PA (1982) Electrostatic potential molecular surfaces. *Proc Natl Acad Sci U S A* 79: 3754-3758.
62. P Politzer, DG Truhlar (1981) *Chemical Application of Atomic and Molecular Electrostatic Potentials*, Plenum, New York.